NUREG/CR--4667-Vol.7

TI90 008482

Environmentally Assisted Cracking in Light Water Reactors

Semiannual Report
April 1988–September 1988

Manuscript Completed: December 1989
Date Published: March 1990

Prepared by
W. J. Shack, T. F. Kassner, J.Y. Park,
W. E. Ruther, W. K. Soppet

Argonne National Laboratory
9700 South Cass Avenue
Argonne, IL 60439

Prepared for
Division of Engineering
Office of Nuclear Regulatory Research
U.S. Nuclear Regulatory Commission
Washington, DC 20555
NRC FIN A2212

Previous Documents in Series

Environmentally Assisted Cracking in Light Water Reactors Annual Report October 1983—September 1984, NUREG/CR-4287, ANL-85-33 (June 1985).

Light-Water-Reactor Safety Materials Engineering Research Programs: Quarterly Progress Report October—December 1984, NUREG/CR-3998 Vol. III, ANL-84-60 Vol. III (October 1985).

Light-Water-Reactor Safety Materials Engineering Research Programs: Quarterly Progress Report January—March 1985, NUREG/CR-4490 Vol. I, ANL-85-75 Vol. I (March 1986).

Environmentally Assisted Cracking in Light Water Reactors Semiannual Report April—September 1985, NUREG/CR-4667 Vol. I, ANL-86-31 (June 1986).

Environmentally Assisted Cracking in Light Water Reactors Semiannual Report October 1985—March 1986, NUREG/CR-4667 Vol. II, ANL-86-37 (September 1987).

Environmentally Assisted Cracking in Light Water Reactors Semiannual Report April—September 1986, NUREG/CR-4667 Vol. III, ANL-87-37 (September 1987).

Environmentally Assisted Cracking in Light Water Reactors Semiannual Report October 1986—March 1987, NUREG/CR-4667 Vol. IV, ANL-87-41 (December 1987).

Environmentally Assisted Cracking in Light Water Reactors Semiannual Report April—September 1987, NUREG/CR-4667 Vol. V, ANL-88-32 (June 1988).

Environmentally Assisted Cracking in Light Water Reactors Semiannual Report October 1987—March 1988, NUREG/CR-4667 Vol. 6, ANL-89-10 (August 1989).

Environmentally Assisted Cracking in Light Water Reactors

by

W. J. Shack, T. F. Kassner, J. Y. Park,
W. E. Ruther, and W. K. Soppet

Abstract

This report summarizes work performed by Argonne National Laboratory on environmentally assisted cracking in light water reactors during the six months from April to September 1988. The stress corrosion cracking (SCC) of Types 316NG and 304 stainless steels (SSs) was investigated by means of slow-strain-rate and fracture-mechanics crack-growth-rate tests in high-temperature water. The effects of load ratio and water chemistry on the crack growth behavior of Type 316NG and sensitized Type 304 SS were determined in long-term fracture-mechanics tests. The influence of organic impurities on the SCC of sensitized Type 304 SS was also investigated. Fatigue tests were conducted on Type 316NG SS in air and simulated boiling water reactor water at 288°C to assess the degree of conservatism in the ASME Code Section III fatigue design curves. An ongoing investigation of the susceptibility of several heats of different grades of low-alloy ferritic steels to transgranular SCC in slow-strain-rate and fracture-mechanics tests was continued.

Contents

List of Tables

List of Figures

Executive Summary

Fracture-mechanics crack-growth-rate (CGR) tests were performed to determine the effect of load ratio and water chemistry (sulfate concentration) on stress corrosion cracking (SCC) of Type 316NG and sensitized Type 304 stainless steel (SS) in oxygenated water. CGR results obtained from numerous tests in this program were compared with predictions of a model that incorporate the effects of water conductivity, electrochemical potential, degree of sensitization, and loading conditions on the rate of crack growth. In general, the model predictions were reasonably consistent with the experimental data.

Additional fatigue tests were performed on Type 316NG SS in air and in simulated boiling water reactor (BWR) water at 288°C for comparison with the ASME Section III design curve and the ASME mean data curve. The results in air agree well with the mean data curve for fairly short lives corresponding to plastic strain ranges greater than 0.5%, but fall below the mean data curve at longer lives. The fatigue life in high-temperature water is about half that in air at a frequency of 0.5 Hz, and the reduction is greater at lower frequencies.

Organic impurities and their decomposition products are a potential concern in BWR water and pressurized water reactor (PWR) secondary-system water in terms of possible increased susceptibility to localized corrosion and SCC of piping and heat-exchanger tube materials. Constant-extension-rate-tensile (CERT) tests were performed on sensitized Type 304 SS specimens in oxygenated (~200 ppb) water containing 1.0 ppm of different organic substances (either oxygen scavengers or several carboxylic acids). As expected, the oxygen scavengers in feedwater decrease to very low levels the effluent oxygen concentration, electrochemical potential (ECP) of the steel, and SCC susceptibility. However, carboxylic acids neither decrease oxygen concentration nor ECP of the steel significantly, but they do reduce SCC susceptibility relative to that observed in high-purity oxygenated water. These species apparently block active sites where cathodic reduction of oxygen occurs and thereby limit anodic dissolution of metal at the crack tip in a slip-dissolution mechanism of crack advance. In SCC tests on fracture-mechanics-type specimens under high-load-ratio, low-frequency cyclic loading conditions at 289°C, the carboxylic acids at a concentration of ~1.0 ppm stop crack growth in the sensitized steel, but are not effective in oxygenated water containing ionic impurities such as sulfate or chloride at the 0.1-ppm level. These results are consistent with the site blockage mechanism for different species that undergo cathodic reduction and control the rate of crack growth of the steel in the SCC tests.

CERT tests were performed on a variety of ferritic steels used for LWR pressure vessels and primary-system piping. Previous results indicated that virtually all of the materials exhibited transgranular SCC (TGSCC) in water containing ~200 ppb dissolved oxygen and 100 ppb sulfate at 289°C. The crack growth rates varied over a wide range (e.g., 10^{-10} to 10^{-8} $m \cdot s^{-1}$), even for the same heat of material. This variation among the different grades of steel and for different heats of the same steel was attributed to the sulfur content and distribution, i.e., materials with fewer sulfide inclusions were less susceptible to TGSCC. Tests performed in water with ~5 to 25 ppb dissolved oxygen and 100 ppb sulfate also showed TGSCC, but the overall CGRs are lower in the low-oxygen environment. The sulfide inclusions act as crack initiation sites.

SCC tests on fracture-mechanics specimens of A533-Gr B steel are in progress. In addition to conventional specimens, some of the specimens were plated with either nickel or gold to reduce contact between the surface of the low-alloy steel and the environment. To simulate crack growth in a clad ferritic steel vessel, composite specimens of A533-Gr B/Inconel-182/Inconel-600 were also fabricated and will be tested.

1 Introduction

Piping in LWR power systems has been affected by several types of environmental degradation. Intergranular stress corrosion cracking (IGSCC) of austenitic SS piping in BWRs has required research, inspection, and mitigation programs that have cost several billion dollars. Because extended lifetimes are envisaged, other potential environmental degradation problems such as corrosion fatigue must be considered. The objective of this program is to develop an independent capability for the assessment of environmentally assisted degradation in LWR systems.

Research during this reporting period focused on (1) SCC of austenitic SS, (2) fatigue of Type 316NG SS, and (3) SCC of ferritic steels used in reactor piping, pressure vessels, and steam generators.

2 Alternative Materials

The objective of this work is to evaluate the resistance of Types 316NG, 347, and CF-3 SS to environmentally assisted cracking in simulated BWR water. These alternative materials for recirculation system piping in BWRs are very resistant to sensitization, and thus are much less susceptible to IGSCC than the Types 304 and 316 SS that are used in many operating reactors. However, their resistance to other modes of degradation, such as TGSCC and corrosion-assisted fatigue, must be evaluated over the range of water chemistries encountered in reactor coolant systems.

Fracture mechanics tests were performed on Types 316NG and 304 SS to better understand the effects of load ratio, R, and water chemistry on crack growth and to help extend the data base for crack growth rates in these materials to cover all the loading histories and water conditions that can occur in operation.

2.1 Technical Progress

2.1.1 Fracture-Mechanics Crack Growth Tests (W. E. Ruther, W. J. Shack, T. F. Kassner, and W. K. Soppet)

Influence of Load-Ratio on the CGR of Types 316NG and 304 SS in Oxygenated (0.2–0.3 ppm) Water

CGR tests were performed on fracture-mechanics specimens of Type 316NG and sensitized 304 SS to assess the effect of different loading conditions on SCC of the steels in high-purity water with 0.2–0.3 ppm dissolved oxygen. The specimens were fatigue precracked in air at 289°C to provide 1-mm-deep starter cracks before testing in water. Crack growth was determined from compliance measurements by means of MTS clip gages attached to the specimens. The tests were conducted under low-frequency cyclic loading at a frequency of 8×10^{-2} Hz and R values of 0.8 to 1.0. Stress intensity values ranged from ~20 to 30 MPa·$m^{1/2}$ for the Type 316NG SS specimen and ~18 to 30 MPa·$m^{1/2}$ for the sensitized Type 304 SS specimen.

The results in Table 1 indicate that cracking did not occur in either specimen over a time interval of ~1080 h at stress intensity factors of ~18–20 MPa·$m^{1/2}$ (Test No. 1). In

Table 1. Crack Growth Results for Type 316NG and Sensitized Type 304 SS Specimens[a] in Oxygenated Water[b] at 289°C in Which the Load Ratio[c] and Stress Intensity Were Varied

Test No.	Time, h	Cond., $\mu S \cdot cm^{-1}$	Electrode Potential		Load Ratio	Type 316NG SS		Type 304 SS	
			304 SS, mV(SHE)	Pt, mV(SHE)		K_{max}[d], $MPa \cdot m^{1/2}$	Growth Rate, $m \cdot s^{-1}$	K_{max}[d], $MPa \cdot m^{1/2}$	Growth Rate, $m \cdot s^{-1}$
1	0 1077	0.12	112 ± 12	182 ± 12	0.95	19.8	~0	17.6	~0
2	1077 2293	0.12	125 ± 10	195 ± 15	0.95	22.6	6.3×10^{-11}	21.2	7.0×10^{-11}
3	2293 3442	0.11	145 ± 10	175 ± 25	0.95	24.4	1.4×10^{-10}	24.2	2.1×10^{-10}
4	3442 4595	0.11	165 ± 5	132 ± 12	1.0	24.5	2.7×10^{-11}	24.5	5.3×10^{-11}
5	4595 5766	0.13	157 ± 12	152 ± 17	0.95	24.6	1.1×10^{-11}	24.7	3.5×10^{-11}
6	5766 6435	0.13	130 ± 20	130 ± 20	0.8	25.7	3.6×10^{-10}	25.2	1.8×10^{-10}
7	6435 7675	0.16	165 ± 25	165 ± 25	0.9	28.5	4.5×10^{-10}	25.4	2.3×10^{-11}
8	7675 9186	0.19	167 ± 17	190 ± 20	1.0	29.0	3.4×10^{-11}	26.0	6.8×10^{-11}
9	9186 10216	0.16	182 ± 12	190 ± 10	0.95	29.0	4.1×10^{-11}	26.1	2.0×10^{-11}
10	10216 12160	0.53[e]	180 ± 20	180 ± 20	0.95	30.0	8.6×10^{-11}	29.9	3.1×10^{-10}

[a] Compact tension specimens (1TCT) of Type 316NG SS (Heat No. P91576; Specimen No. E04) and Type 304 SS (Heat No. 30956; Specimen No. 21) with the following heat treatments: solution-anneal at 1050°C for 0.5 h plus 650°C for 24 h for the Type 316NG SS (EPR = 0 $C \cdot cm^{-2}$), and solution anneal at 1050°C for 0.5 h followed by 700°C for 0.25 h plus 500°C for 24 h for the Type 304 SS (EPR = 2 $C \cdot cm^{-2}$).

[b] Effluent dissolved-oxygen concentration was 0.2–0.3 ppm; feedwater oxygen concentration was approximately a factor of 2 higher to compensate for oxygen depletion by corrosion of the autoclave system.

[c] Frequency of the positive sawtooth waveform was 8×10^{-2} Hz.

[d] Stress intensity, K_{max}, values at the end of the time period.

[e] Sulfate (0.05 ppm as H_2SO_4) was added to the feedwater.

Test No. 2, cracking occurred in both specimens at a rate of ~7 x 10^{-11} m·s^{-1} at a stress intensity factor of ~21–23 MPa·$m^{1/2}$, which apparently represents the threshold stress intensity value in high-purity water at 289°C. When the stress intensity factor was raised to ~24 MPa·$m^{1/2}$ in Test No. 3, the CGRs increased by a factor of ~2–3. When the load ratio was increased from 0.95 to 1.0 (constant load) in Test No. 4, the CGRs decreased by a factor of 4–5. The rates decreased further when the load ratio was returned to the previous value of 0.95 in Test No. 5. In Test No. 6, the load ratio was decreased to 0.8 and the CGR of both specimens increased by an order of magnitude to 3.6 x 10^{-10} and 1.8 x 10^{-10} m·s^{-1} for the Type 316NG and 304 SS specimens, respectively. An increase in the load ratio from 0.8 to 0.9 in Test No. 7 caused a significant decrease in the CGR of the Type 304 SS specimen to a value of 2.3 x 10^{-11} m·s^{-1}, but the CGR of the Type 316NG SS specimen was not affected. When the load ratio was once again increased to 1.0, Test No. 8, the CGRs decreased to approximately the same values as in Test No. 4 even though the stress intensity values were somewhat higher. When the load ratio was decreased to a value of 0.95 in Test No. 9, the CGR of the Type 316NG SS specimen was relatively unaffected (increased slightly) and that of the Type 304 SS specimen decreased, as was the situation in Test No. 5. In the last test (No. 10), 50 ppb sulfate was added to the feedwater, and the CGRs of both specimens increased by factors of ~2 and 15, respectively. A greater sensitivity of the CGR of sensitized Type 304 SS to sulfate additions, in comparison with that of Type 316NG SS, has been observed in many other tests. A more systematic study of the influence of sulfate at low concentrations (0–100 ppb) on the SCC behavior of these steels is reported in the following section. The results in Table 1 indicate that the CGRs of the two steels are strongly dependent on load ratio and probably the load history, but are relatively independent of the stress intensity value in the range of ~22 to 30 MPa·$m^{1/2}$.

Figure 1 shows the morphology of the fatigue and stress corrosion cracks in the two specimens. The 1TCT specimens were sectioned vertically, and half of each specimen was split in the plane of the crack in liquid-nitrogen. The corrosion product film was removed from the fracture surface by a chemical process to reveal the morphology of the underlying material. The intact portion of the specimen that encompassed the crack was polished and etched to corroborate the mode of crack propagation and also to determine if crack branching had occurred during the test. The total crack lengths at the end of the test were compared with values obtained from the clip gages. A typical intergranular fracture morphology is evident in the lightly sensitized Type 304 SS specimen (No. 21). Scanning electron microscopy evaluation of the fracture surface of the Type 316NG specimen (No. E-04) indicated a transition from a transgranular to an intergranular crack path near the end of the test at crack depth of ~6 mm into the specimen. The intergranular nature of the crack in the crack-tip region can be seen in the left-hand micrograph of the cross-section.

Influence of Sulfate and Chromate at Low Concentrations (<100 ppb) in Oxygenated (0.2–0.3 ppm) Water on the CGR of Types 316NG and 304 SS

Fracture-mechanics CGR tests on Types 316NG and 304 SS were performed to help quantify the beneficial effects of improved water purity. The tests were performed on sensitized (EPR = 2 C/cm^2) Type 304 SS and a Type 316NG SS specimens at 289°C in water with 0.2–0.3 ppm dissolved oxygen at a load ratio of 0.95, a frequency of 0.08 Hz, and a K_{max} of ~30 MPa·$m^{1/2}$. The tests were initiated in oxygenated water with 100 ppb sulfate (as H_2SO_4) at a conductivity of 0.9 μS·cm^{-1} (Test No. 1) and the impurity level was varied

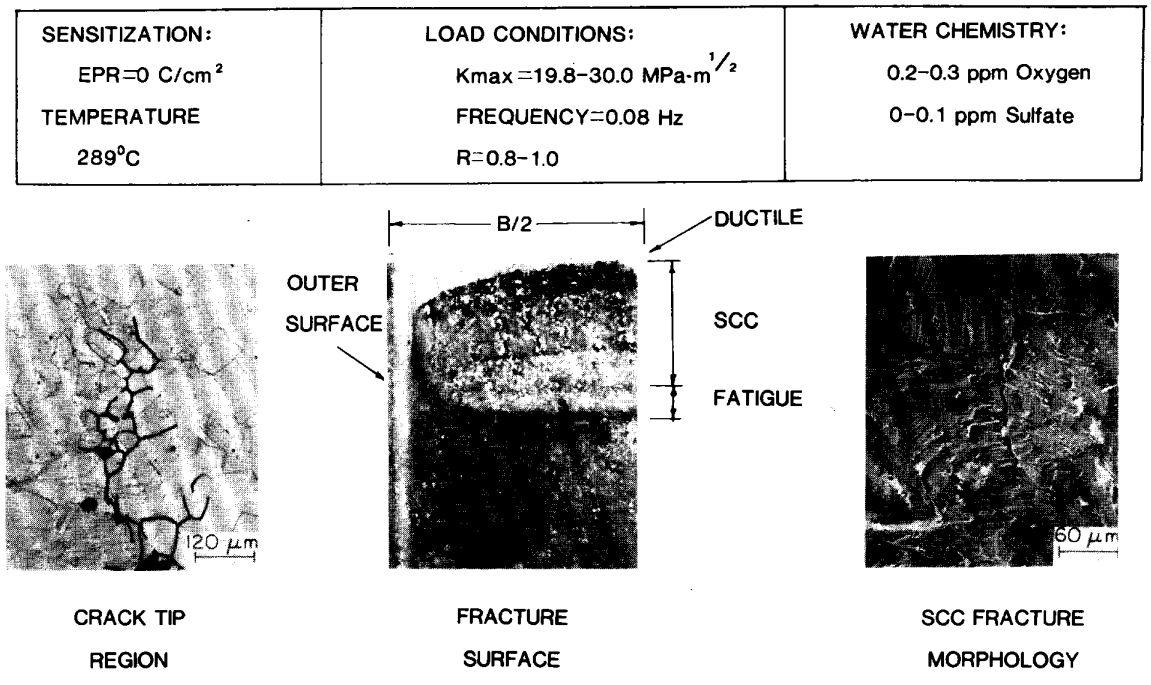

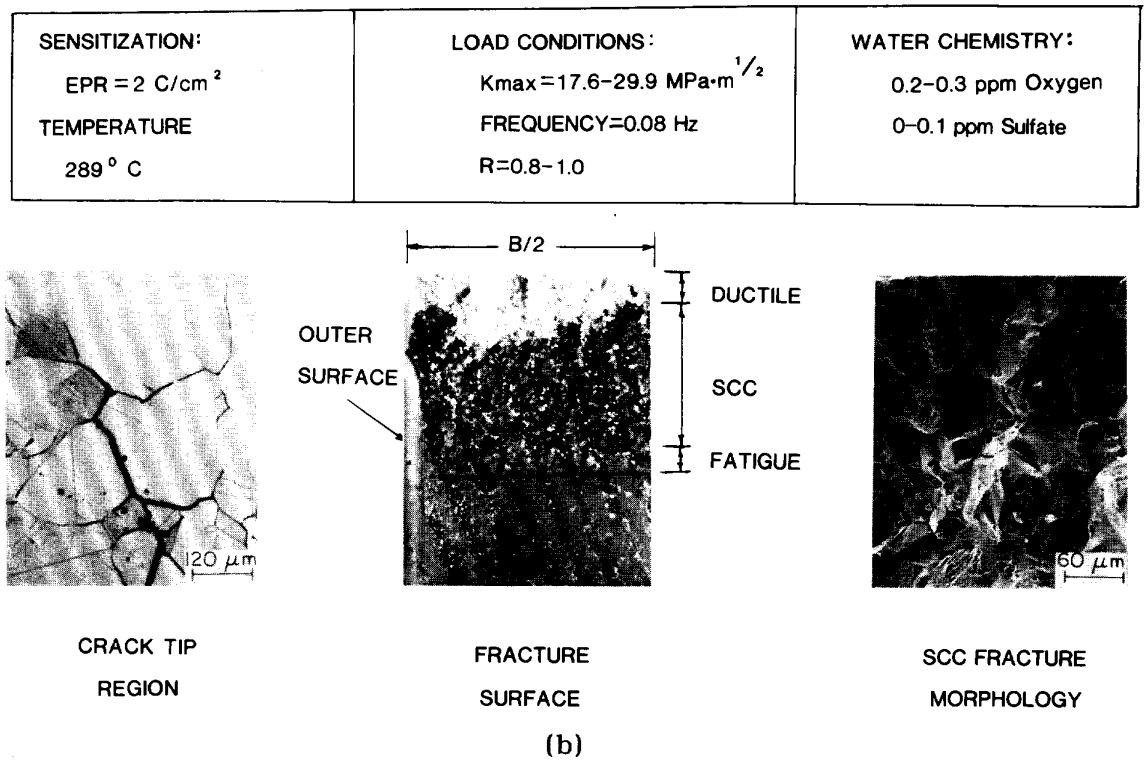

Figure 1. Fracture Surface and SCC Fracture Morphology of 1TCT Specimens of (a) Type 316NG (Specimen No. E-04) and (b) Sensitized Type 304 SS (Specimen No. 21) after a Crack Growth Experiment at 289°C without and with Low Levels of Sulfate in the Oxygenated Feedwater.

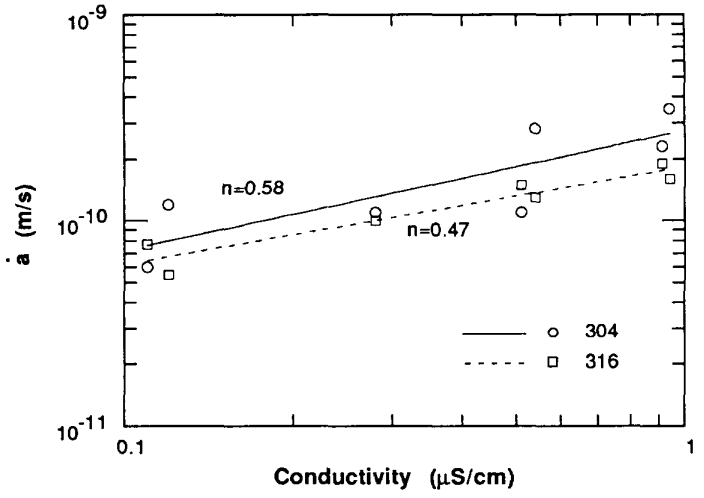

Figure 2.
Crack Growth Rates of 1TCT Specimens of Type 316NG and Sensitized (EPR = 2 C/cm^2) Type 304 SS as a Function of Conductivity of Water Containing 0 to 100 ppb Sulfate and ~200 ppb Dissolved Oxygen at 289°C.

during Test Nos. 2 to 8 to obtain conductivity values between 0.1 and 0.9 $\mu S \cdot cm^{-1}$. In Test No. 9, 25 ppb chromate (as H_2CrO_4) was added to the feedwater to determine it's effect in comparison with that of sulfate at the same concentration. The CGRs at different impurity concentrations in the feedwater are given in Table 2 and the values are plotted as a function of conductivity in Fig. 2.

As expected, the CGRs of sensitized Type 304 SS decrease with improvement of the water quality (Test Nos. 2 to 5). The larger CGR values in Test No. 3 can be attributed to the lower R value (0.92 versus 0.95) in this test, which is consistent with the results in the previous section. Data from earlier work[1] suggest that a "threshold" impurity effect marked by a sharp decrease in crack growth rate ȧ may exist at a very low conductivity level, but for the range of conductivities in the tests in Table 2 and Fig. 2, the dependence of ȧ on conductivity is fairly weak. An empirical fit to the data gives a power-law dependence on conductivity of ~0.5. The results are consistent with the behavior observed in CERTs at a low dissolved oxygen concentration with sulfate additions in the range of 0.1–10 ppm.[1] The CGRs of the steels in oxygenated water containing 25 ppb of chromate and sulfate are the same, within the uncertainty of the measurements. When these species were not added to the feedwater (Test Nos. 10 and 8, respectively), the CGR of the sensitized Type 304 SS specimen decreased to a very low value, whereas that of the Type 316NG SS specimen was not affected by the improvement in water quality. This difference in the relative response of the two materials to a transition to high-purity water has been observed in many previous tests.

Comparison of CGR Data for Types 316NG and 304 SS in Oxygenated (0.2–0.3 ppm) Water Containing 0–100 ppb Sulfate with Model Predictions

To compare our CGR data on these steels in simulated BWR water with various models for crack growth in high-temperature water, a data base was compiled from the results obtained to date in this program. Tables 3–5 summarize the results in high-purity water containing 0.2 to 0.3 and 7 to 8 ppm oxygen, and in oxygenated water (0.2–0.3 ppm) with ≤100 ppb sulfate at 289°C. For completeness, the recent data from Tables 1 and 2 are also included in Tables 3 and 5.

Table 2. Crack Growth Results under High-R Loading[a] for Type 316NG and Sensitized Type 304 SS Specimens[b] in Oxygenated Water[c] at 289°C in Which the Sulfate Concentration Was Varied

Test No.	Time, h	Water Chemistry: Conc., ppb	Water Chemistry: Cond., $\mu S \cdot cm^{-1}$	Water Chemistry: pH at 25°C	Electrode Potential: 304 SS, mV(SHE)	Electrode Potential: Pt, mV(SHE)	Type 316NG SS: K_{max}[d], $MPa \cdot m^{1/2}$	Type 316NG SS: Growth Rate, $m \cdot s^{-1}$	Type 304 SS: K_{max}[d], $MPa \cdot m^{1/2}$	Type 304 SS: Growth Rate, $m \cdot s^{-1}$
1	0 1162	100	0.91	5.80	110	194	28.6	1.9×10^{-10}	30.0	2.3×10^{-10}
2	1162 1472	50	0.51	5.94	162	218	28.8	1.5×10^{-10}	30.2	1.1×10^{-10}
3	1472 2163	50	0.51	5.94	162	218	30.5[e]	4.3×10^{-10}	32.0[e]	4.5×10^{-10}
4	2163 2932	25	0.28	6.02	145	199	31.0	1.0×10^{-10}	32.6	1.1×10^{-10}
5	2932 3814	–	0.12	6.58	145	174	31.4	0.6×10^{-10}	33.4	1.2×10^{-10}
6	3814 4826	50	0.54	5.98	117	194	32.1	1.3×10^{-10}	35.4	2.8×10^{-10}
7	4826 6111	100	0.94	5.75	138	209	33.2	1.6×10^{-10}	39.7	3.5×10^{-10}
8	6111 6867	–	0.11	6.33	108	179	33.6	0.8×10^{-10}	39.9	~0
9	6867 8130	[f]	0.21	6.20	100	179	34.6	1.7×10^{-10}	40.6	1.1×10^{-10}
10	8130 8946	–	0.15	6.27	95	95	35.4	1.5×10^{-10}	40.7	0.2×10^{-10}

[a] R value of 0.95 and frequency of the positive sawtooth waveform of 8×10^{-2} Hz.

[b] Compact tension specimens (1TCT) of Type 316NG SS (Heat No. P91576; Specimen No. CPT9-2) and Type 304 SS (Heat No. 30956; Specimen No. 31) with the following heat treatments: solution-anneal at 1050°C for 0.5 h plus 650°C for 24 h for the Type 316NG SS (EPR = 0 $C \cdot cm^{-2}$), and solution-anneal at 1050°C for 0.5 h followed by 700°C for 0.25 h plus 500°C for 24 h for the Type 304 SS (EPR = 2 $C \cdot cm^{-2}$).

[c] Effluent dissolved-oxygen concentration was 0.2–0.3 ppm; feedwater oxygen concentration was approximately a factor of 2 higher to compensate for oxygen depletion by corrosion of the autoclave system.

[d] Stress intensity, K_{max}, values at the end of the time period.

[e] R value was 0.92 in this test.

[f] Chromate (25 ppb as H_2CrO_4) was added to the feedwater.

Table 3. Summary of Crack Growth Results for Type 316NG and Sensitized and Solution Annealed Type 304 SS Specimens[a] in Oxygenated (~200 ppb) Water[b] at 289°C in Which the Load Ratio[c] and Stress Intensity Were Varied

	Electrode Potential			Type 316NG SS			Type 304 SS					
Cond., $\mu S \cdot cm^{-1}$	304 SS, mV(SHE)	Pt, mV(SHE)	Load Ratio	K_{max}[d], $MPa \cdot m^{1/2}$	ΔK, $MPa \cdot m^{1/2}$	Growth Rate, $m \cdot s^{-1}$	K_{max}[d], $MPa \cdot m^{1/2}$	ΔK, $MPa \cdot m^{1/2}$	Growth Rate, $m \cdot s^{-1}$	EPR, $C \cdot cm^{-2}$	Ref. No.	ANL No.
0.11	–	–	0.95	–	–	–	27.3	1.37	1.0×10^{-10}	0	2	83-85 IV
0.11	–	–	0.95	–	–	–	29.3	1.46	3.3×10^{-10}	2	2	83-85 IV
0.11	–	–	0.95	–	–	–	29.9	1.50	3.0×10^{-10}	20	2	83-85 IV
0.16	–	–	0.95	–	–	–	28.0	1.40	1.8×10^{-10}	0	2	83-85 IV
0.16	–	–	0.95	–	–	–	30.3	1.51	0.4×10^{-10}	2	2	83-85 IV
0.16	–	–	0.95	–	–	–	31.3	1.56	2.8×10^{-10}	20	2	83-85 IV
0.14	–	–	0.95	–	–	–	28.4	1.42	1.6×10^{-10}	0	2	83-85 IV
0.14	–	–	0.95	–	–	–	31.5	1.57	2.5×10^{-10}	2	2	83-85 IV
0.14	–	–	0.95	–	–	–	31.9	1.59	2.2×10^{-10}	20	2	83-85 IV
0.15	–	–	0.95	–	–	–	31.2	1.56	1.7×10^{-10}	0	3	85-33
0.15	–	–	0.95	–	–	–	36.5	1.83	2.5×10^{-10}	2	3	85-33
0.15	–	–	0.95	–	–	–	38.4	1.92	8.4×10^{-11}	2	3	85-33
0.15	–	–	0.95	–	–	–	35.4	1.77	2.1×10^{-10}	20	3	85-33
0.15	–	–	0.95	–	–	–	36.8	1.84	5.1×10^{-11}	20	3	85-33
0.10	138 ± 12	219 ± 10	0.95	31.2	1.56	1.4×10^{-10}	33.6	1.68	0	2	4	87-37
0.10	115 ± 15	230 ± 15	0.95	33.7	1.68	2.1×10^{-10}	34.9	1.75	0	2	4	87-37
0.10	145 ± 10	220 ± 10	0.95	34.1	1.70	5.0×10^{-11}	36.2	1.81	1.3×10^{-10}	2	4	87-37
0.10	140 ± 10	210 ± 10	0.95	34.6	1.73	4.0×10^{-11}	37.1	1.86	7.0×10^{-11}	2	4	87-37
0.21	95 ± 10	110 ± 10	0.95	–	–	–	29.7	1.49	1.7×10^{-10}	2	5	87-41
0.13	75 ± 10	–	0.95	32.1	1.61	3.0×10^{-10}	–	–	–	–	6	88-32
0.12	80 ± 10	85 ± 10	0.95	32.2	1.61	2.5×10^{-11}	–	–	–	–	6	88-32
0.15	140 ± 10	160 ± 15	0.95	33.2	1.66	1.1×10^{-10}	–	–	–	–	6	88-32
0.20	170 ± 10	190 ± 15	0.95	30.5	1.53	2.2×10^{-10}	28.8	1.44	2.0×10^{-10}	2	7	89-10
0.20	170 ± 10	205 ± 15	0.95	33.0	1.65	2.0×10^{-10}	29.9	1.50	1.2×10^{-10}	2	7	89-10
0.11	165 ± 5	132 ± 12	1.00	24.5	0.00	2.7×10^{-11}	24.5	0.00	5.3×10^{-11}	2	–[e]	89-40
0.19	167 ± 17	190 ± 20	1.00	29.0	0.00	3.4×10^{-11}	26.0	0.00	6.8×10^{-11}	2	–[e]	89-40
0.12	112 ± 12	182 ± 12	0.95	19.8	0.96	~0	17.6	0.87	~0	2	–[e]	89-40
0.12	125 ± 10	195 ± 15	0.95	22.6	1.13	6.3×10^{-11}	21.2	1.06	7.0×10^{-11}	2	–[e]	89-40

Continued on next page

Table 3. (Continued)

Cond., $\mu S \cdot cm^{-1}$	Electrode Potential: 304 SS, mV(SHE)	Electrode Potential: Pt, mV(SHE)	Load Ratio	Type 316NG SS: K_{max}[d], $MPa \cdot m^{1/2}$	Type 316NG SS: ΔK, $MPa \cdot m^{1/2}$	Type 316NG SS: Growth Rate, $m \cdot s^{-1}$	Type 304 SS: K_{max}[d], $MPa \cdot m^{1/2}$	Type 304 SS: ΔK, $MPa \cdot m^{1/2}$	Type 304 SS: Growth Rate, $m \cdot s^{-1}$	Type 304 SS: EPR, $C \cdot cm^{-2}$	Ref. No.	ANL No.
0.11	145 ± 10	175 ± 25	0.95	24.4	1.22	1.4×10^{-10}	24.2	1.21	2.1×10^{-10}	2	–[e]	89-40
0.13	157 ± 12	152 ± 17	0.95	24.6	1.23	1.1×10^{-11}	24.7	1.23	3.5×10^{-11}	2	–[e]	89-40
0.16	182 ± 12	190 ± 10	0.95	29.0	1.45	4.1×10^{-11}	26.1	1.30	2.0×10^{-11}	2	–[e]	89-40
0.16	165 ± 25	165 ± 25	0.90	28.5	2.85	4.5×10^{-10}	25.4	2.54	2.3×10^{-11}	2	–[e]	89-40
0.13	130 ± 20	130 ± 20	0.80	25.7	5.12	3.6×10^{-10}	25.2	5.03	1.8×10^{-10}	2	–[e]	89-40
0.12	145	174	0.95	31.4	1.57	6.0×10^{-11}	33.4	1.67	1.2×10^{-10}	2	–[f]	89-40
0.11	108	179	0.95	33.6	1.68	8.0×10^{-11}	39.9	2.00	~0	2	–[f]	89-40
0.15	95	95	0.95	35.4	1.77	1.5×10^{-10}	40.7	2.04	2.0×10^{-11}	2	–[f]	89-40
0.13	195	200	0.95	–	–	–	30.4	1.52	2.9×10^{-10}	2	–[g]	89-40
0.12	190	200	0.95	–	–	–	33.6	1.68	2.9×10^{-10}	2	–[g]	89-40

[a] Compact tension specimens (1TCT) of Type 316NG SS (Heat No. P91576) and Type 304 SS (Heat No. 30956) with the following heat treatments: solution anneal at 1050°C for 0.5 h plus 650°C for 24 h for the Type 316NG SS (EPR = 0 $C \cdot cm^{-2}$), and solution anneal at 1050°C for 0.5 h (EPR = 0 $C \cdot cm^{-2}$) followed by 700°C for 0.25 h plus 500°C for 24 h (EPR = 2 C/cm^2) or 700°C for 12 h (EPR = 20$C \cdot cm^{-2}$) for the Type 304 SS.

[b] Effluent dissolved-oxygen concentration was 0.2–0.3 ppm; feedwater oxygen concentration was approximately a factor of 2 higher to compensate for oxygen depletion by corrosion of the autoclave systems.

[c] Frequency of the positive sawtooth waveform was 8×10^{-2} Hz.

[d] Stress intensity, K_{max}, values at the end of a ~1000-h time period of steady-state crack growth.

[e] Table 1 of this report.

[f] Table 2 of this report.

[g] Table 13 of this report.

Table 4. Summary of Crack Growth Results for Sensitized Type 304 SS Specimens[a] in Oxygenated (~8 ppm) Water[b] at 289°C in Which the Load Ratio, Frequency[c], and Stress Intensity Were Varied

Cond., $\mu S \cdot cm^{-1}$	Potential 304 SS, mV(SHE)	Load Ratio	Freq., Hz	Type 304 SS K_{max}[d], $MPa \cdot m^{1/2}$	Type 304 SS ΔK, $MPa \cdot m^{1/2}$	Type 304 SS Growth Rate, $m \cdot s^{-1}$	EPR, $C \cdot cm^{-2}$	Ref. No.	ANL No.
<0.2	–	1.0	0	34.0	0	1.2×10^{-10}	1.4	8	84-60 III
<0.2	–	1.0	0	37.0	0	2.9×10^{-10}	1.4	8	84-60 III
<0.2	–	1.0	0	38.0	0	4.5×10^{-10}	1.4	8	84-60 III
<0.2	–	1.0	0	33.0	0	2.2×10^{-10}	1.8	8	84-60 III
<0.2	–	1.0	0	29.0	0	1.8×10^{-10}	HAZ	9	85-75 I
<0.2	–	0.95	8×10^{-2}	28.0	1.40	7.5×10^{-10}	20	10	83-85 II
<0.2	–	0.95	8×10^{-2}	34.0	1.70	1.0×10^{-9}	20	10	83-85 II
<0.2	–	0.95	8×10^{-2}	35.0	1.75	1.2×10^{-9}	20	10	83-85 II
<0.2	–	0.95	8×10^{-3}	34.0	1.70	1.2×10^{-10}	20	10	83-85 II
<0.2	–	0.95	8×10^{-3}	38.0	1.90	1.5×10^{-10}	20	10	83-85 II
<0.2	–	0.95	8×10^{-3}	50.0	2.50	4.7×10^{-10}	20	10	83-85 II
<0.2	–	0.95	8×10^{-3}	61.0	3.04	1.1×10^{-9}	20	10	83-85 II
<0.2	–	0.95	8×10^{-3}	64.0	3.20	1.7×10^{-9}	20	10	83-85 II
<0.2	–	0.95	8×10^{-4}	28.0	1.40	1.2×10^{-10}	20	10	83-85 II
<0.2	–	0.95	8×10^{-4}	67.0	3.35	1.9×10^{-9}	20	10	83-85 II
<0.2	–	0.95	8×10^{-4}	70.0	3.50	3.2×10^{-9}	20	10	83-85 II
<0.2	–	0.95	8×10^{-4}	72.0	3.60	3.3×10^{-9}	20	10	83-85 II
<0.2	–	0.95	2×10^{-3}	36.0	1.70	1.5×10^{-10}	1.4	8	84-60 III
<0.2	–	0.95	2×10^{-3}	37.0	1.85	1.5×10^{-10}	1.4	8	84-60 III
<0.2	–	0.95	2×10^{-3}	39.0	1.95	2.0×10^{-10}	1.4	8	84-60 III
<0.2	–	0.95	2×10^{-3}	40.0	2.00	3.1×10^{-10}	1.4	8	84-60 III
<0.2	–	0.95	2×10^{-3}	28.0	1.40	2.2×10^{-10}	HAZ	9	85-75 I
<0.2	–	0.94	1×10^{-1}	31.0	1.86	3.1×10^{-10}	1.4	8	84-60 III
<0.2	–	0.94	1×10^{-1}	32.0	1.92	1.9×10^{-10}	1.4	8	84-60 III
<0.2	–	0.94	1×10^{-1}	30.0	1.80	2.1×10^{-10}	1.8	8	84-60 III
<0.2	–	0.90	2×10^{-3}	28.0	2.80	1.3×10^{-10}	HAZ	9	85-75 I
<0.2	–	0.80	2×10^{-3}	29.0	5.80	6.6×10^{-10}	HAZ	9	85-75 I
<0.2	–	0.80	2×10^{-3}	31.0	6.20	4.4×10^{-10}	1.4	8	84-60 III
<0.2	–	0.80	2×10^{-3}	32.0	6.39	7.4×10^{-10}	1.4	8	84-60 III
<0.2	–	0.79	2×10^{-3}	32.0	6.70	5.5×10^{-10}	1.4	8	84-60 III
<0.2	–	0.79	2×10^{-3}	36.0	7.55	5.4×10^{-10}	1.4	8	84-60 III

Continued on next page

Table 4. (Continued)

Cond., $\mu S \cdot cm^{-1}$	Potential 304 SS, mV(SHE)	Load Ratio	Freq., Hz	Type 304 SS K_{max}[d], $MPa \cdot m^{1/2}$	ΔK, $MPa \cdot m^{1/2}$	Growth Rate, $m \cdot s^{-1}$	EPR, $C \cdot cm^{-2}$	Ref. No.	ANL No.
<0.2	–	0.70	2×10^{-3}	31.0	9.30	3.4×10^{-10}	1.4	8	84-60 III
<0.2	–	0.70	2×10^{-3}	33.0	9.90	5.9×10^{-10}	1.4	8	84-60 III
<0.2	–	0.60	2×10^{-3}	29.0	11.60	5.6×10^{-9}	1.8	8	84-60 III
<0.2	–	0.60	2×10^{-3}	33.0	13.20	6.6×10^{-10}	1.4	8	84-60 III
<0.2	–	0.50	1×10^{-3}	32.0	16.00	2.6×10^{-10}	1.4	8	84-60 III
<0.2	–	0.50	2×10^{-3}	31.0	15.50	8.9×10^{-10}	1.4	8	84-60 III
<0.2	–	0.50	2×10^{-3}	33.0	16.50	3.4×10^{-9}	1.4	8	84-60 III
<0.2	–	0.50	2×10^{-3}	32.0	16.00	2.8×10^{-9}	1.8	8	84-60 III

[a] Compact tension specimens (1TCT) of Type 304 SS with the following heat treatments: Heat No.10285, solution anneal at 1050°C for 0.5 h plus 700°C/10 min and 450°C/146 h or 450°C/250 h (EPR = 1.4 $C \cdot cm^{-2}$), or 500°C/24 h (EPR = 1.8 $C \cdot cm^{-2}$). Heat No. 30956 solution anneal at 1050°C for 0.5 h followed by 700°C for 12 h (EPR = 20 $C \cdot cm^{-2}$). HAZ specimen was fabricated from a weld overlay applied to a 12-in. diam pipe.

[b] Effluent dissolved-oxygen concentration was 7-8 ppm.

[c] Positive sawtooth waveform was used.

[d] Stress intensity, K_{max}, values at the end of a ~500 to 1000-h time period of steady-state crack growth.

Table 5. Summary of Crack Growth Results for Type 316NG and Sensitized and Solution Annealed Type 304 SS Specimens[a] in Oxygenated (~200 ppb) Water[b] with <100 ppb Sulfate at 289°C in Which the Load Ratio[c] and Stress Intensity Were Varied

		Potential			Type 316NG SS			Type 304 SS					
Cond., $\mu S \cdot cm^{-1}$	SO_4^{2-}, ppb	304 SS, mV(SHE)	Pt, mV(SHE)	Load Ratio	K_{max}[d], $MPa \cdot m^{1/2}$	ΔK, $MPa \cdot m^{1/2}$	Growth Rate,[e] $m \cdot s^{-1}$	K_{max}[d], $MPa \cdot m^{1/2}$	ΔK, $MPa \cdot m^{1/2}$	Growth Rate,[f] $m \cdot s^{-1}$	EPR, $C \cdot cm^{-2}$	Ref. No.	ANL No.
0.92	100	–	–	0.95	–	–	–	42.1	2.10	6.1×10^{-10}	0	2	83-85 IV
1.04	100	–	–	0.95	–	–	–	49.8	2.49	6.9×10^{-10}	0	2	83-85 IV
0.92	100	–	–	0.95	–	–	–	53.2	2.66	6.4×10^{-10}	2	2	83-85 IV
1.04	100	–	–	0.95	–	–	–	63.4	3.17	1.6×10^{-9}	2	2	83-85 IV
0.92	100	–	–	0.95	–	–	–	42.0	2.10	1.6×10^{-10}	20	2	83-85 IV
1.04	100	–	–	0.95	–	–	–	42.2	2.11	1.0×10^{-10}	20	2	83-85 IV
0.88	100	80	180	0.95	–	–	–	26.5	1.33	2.8×10^{-10}	0	9	85-75 I
0.88	100	120	215	0.95	–	–	–	28.1	1.41	4.2×10^{-10}	0	9	85-75 I
0.88	100	120	190	0.95	–	–	–	32.3	1.62	4.2×10^{-10}	0	9	85-75 I
0.88	100	80	180	0.95	–	–	–	27.0	1.35	5.0×10^{-10}	2	9	85-75 I
0.88	100	120	215	0.95	–	–	–	30.0	1.50	3.4×10^{-10}	2	9	85-75 I
0.88	100	120	190	0.95	–	–	–	32.4	1.62	2.9×10^{-10}	2	9	85-75 I
0.88	100	80	180	0.95	–	–	–	27.1	1.36	4.2×10^{-10}	20	9	85-75 I
0.88	100	120	215	0.95	–	–	–	29.3	1.46	3.4×10^{-10}	20	9	85-75 I
0.88	100	120	190	0.95	–	–	–	31.4	1.57	2.6×10^{-10}	20	9	85-75 I
0.86	100	120	225	0.95	29.7	1.49	1.7×10^{-10}	31.6	1.58	2.3×10^{-10}	2	4	87-37
0.88	100	120	190	0.95	32.2	1.61	1.9×10^{-10}	33.8	1.69	3.2×10^{-10}	2	4	87-37
0.29	30	145	230	0.95	36.3	1.82	1.3×10^{-10}	38.9	1.95	6.0×10^{-11}	2	4	87-37
0.35	30	85	90	0.95	28.0	1.40	~0	32.1	1.61	2.2×10^{-10}	2	5	87-41
0.93	100	65	65	0.95	–	–	–	34.3	1.72	4.4×10^{-10}	2	5	87-41
0.93	100	115	130	0.95	–	–	–	42.6	2.14	8.0×10^{-10}	2	5	87-41
0.80	100	190	220	0.95	34.4	1.72	7.9×10^{-11}	–	–	–	–	6	88-32
0.77	g	200	215	0.95	33.7	1.68	8.4×10^{-11}	–	–	–	–	6	88-32
0.53	50	180	180	0.95	30.0	1.50	8.6×10^{-11}	29.9	1.50	3.1×10^{-10}	2	–[h]	89-40
0.91	100	110	194	0.95	28.6	1.43	1.9×10^{-10}	30.0	1.50	2.3×10^{-10}	2	–[i]	89-40
0.51	50	162	218	0.95	28.8	1.44	1.5×10^{-10}	30.2	1.51	1.1×10^{-10}	2	–[i]	89-40
0.28	25	145	199	0.95	31.0	1.55	1.0×10^{-10}	32.6	1.63	1.1×10^{-10}	2	–[i]	89-40
0.54	50	117	194	0.95	32.1	1.61	1.3×10^{-10}	35.4	1.77	2.8×10^{-10}	2	–[i]	89-40
0.94	100	138	209	0.95	33.2	1.66	1.6×10^{-10}	39.7	1.99	2.3×10^{-10}	2	–[i]	89-40
0.21	j	100	179	0.95	34.6	1.73	1.7×10^{-10}	40.6	2.03	2.0×10^{-11}	2	–[i]	89-40
0.51	50	162	218	0.92	30.5	2.44	4.3×10^{-10}	32.0	2.56	4.5×10^{-10}	2	–[i]	89-40

[a] Compact tension specimens (1TCT) of Type 316NG SS (Heat No. P91576) and Type 304 SS (Heat No. 30956) with the following heat treatments: solution anneal at 1050°C for 0.5 h plus 650°C for 24 h for the Type 316NG SS (EPR = 0 $C \cdot cm^{-2}$), and solution anneal at 1050°C for 0.5 h (EPR = 0 $C \cdot cm^{-2}$) followed by 700°C for 0.25 h plus 500°C for 24 h (EPR = 2 $C \cdot cm^{-2}$) or 700°C for 12 h (EPR = 20 $C \cdot cm^{-2}$) for the Type 304 SS.

[b] Effluent dissolved-oxygen concentration was 0.2–0.3 ppm; feedwater oxygen concentration was approximately a factor of 2 higher to compensate for oxygen depletion by corrosion of the autoclave systems.

[c] Frequency of the positive sawtooth waveform was 8×10^{-2} Hz.

[d] Stress intensity, K_{max}, values at the end of a ~1000-h time period of steady-state crack growth.

[e] Cracking was transgranular, i.e., TGSCC.

[f] Cracking was intergranular, i.e., IGSCC.

[g] Nitric acid was added to the feedwater (~100 ppb).

[h] Table 1 of this report.

[i] Table 2 of this report.

[j] Chromate was added to the feedwater (~25 ppb as H_2CrO_4).

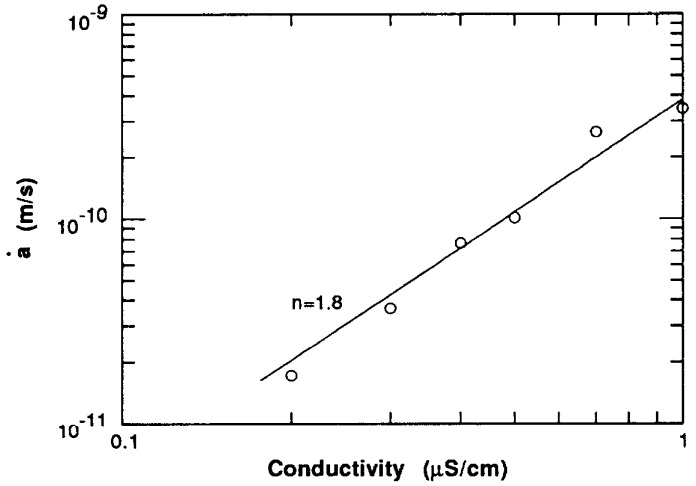

Figure 3.
Predicted Dependence of the CGRs of Sensitized (EPR = 15 C/cm²) Type 304 SS on Conductivity at an ECP Value of 100 mV(SHE) According to the Model of Ford et al.[11]

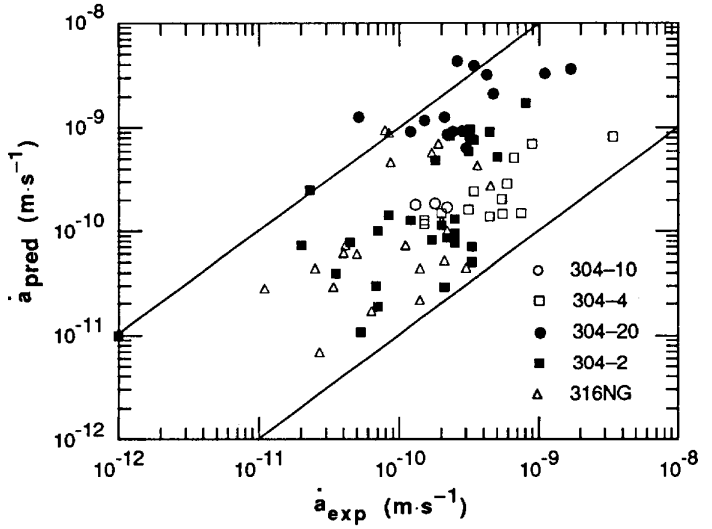

Figure 4.
Comparison of Predicted and Measured CGRs for 85 Tests[2-10] *on Types 316NG and 304 SS at Sulfate Levels of 0 to 100 ppb, R values of 0.8 to 1.0, and Stress Intensity Values of 18 to 64 MPa·m$^{1/2}$.*

Predictions of SCC growth rates from a model developed by Ford et al.[11] are compared with experimental results in Figs. 3 and 4. Although the CGR dependence on conductivity is not given explicitly in the model, parametric calculations show that over the range of conductivities of interest, e.g., 0.1–1.0 μS·cm^{-1}, the effective power-law dependence on conductivity is typically 1.0–1.9. The predicted behavior of sensitized Type 304 SS (EPR=15 C/cm^2) at an electrochemical potential of 100 mV(SHE) is shown in Fig. 3. The effective power-law dependence in this case is 1.8. In Fig. 4, predictions from the model are compared with results from 85 CGR tests on Types 304 and 316NG SS at sulfate levels of 0–100 ppb, R values of 0.8–1.0, and stress intensity values of 18–64 MPa·m$^{1/2}$ from the data base in Tables 3 and 5. In almost all cases, the model predictions are within a factor of 10 of the experimental results. However, as mentioned previously, the model predicts a stronger dependence of the CGRs on impurity level than is observed in these tests.

2.1.2 Fatigue of Type 316NG SS (W. J. Shack and W. F. Burke)

Residual-life assessment reviews for LWRs indicate that low-cycle fatigue is a potentially significant degradation mechanism in LWR primary piping and must be considered when justifying extended operation of an LWR plant.[12] Current fatigue design for austenitic SS piping is based on the ASME Section III Fatigue Design Curves. Environmental effects are not explicitly considered in these curves. Instead, the design curves are obtained by introducing a factor of 2 on the strain range or 20 on the cycles from the mean life curve, whichever is more conservative. Several studies[13,14] have shown that the effect of the standard BWR environment on the fatigue life of A106-Gr B and A333-Gr 6 steel can completely erode the "2 or 20" margin in the Code Design Curve.

The objective of the current work is to provide additional information on the effects of operating temperature and environment on the fatigue behavior of Type 316NG SS. The data are needed to assess the degree of conservatism inherent in the ASME Code Section III Fatigue Design Curves for this material. They may also be needed for decisions on life extension beyond the current 40-year design life.

Type 316NG SS test specimens were fabricated from a segment of 22-in.-diam pipe manufactured by Sumitomo for the new recirculation piping system installed at the Cooper BWR. No additional heat treatment was performed so that the condition of the material is as close as possible to the actual piping. Baseline in-air tests were performed with the same specimen design and loading systems that were used for the tests in simulated BWR water. The tests in air were performed under strain control where the strain in the specimen was measured with an axial extensometer. The specimen stroke was monitored during these tests.

Because it is difficult to monitor specimen strain in tests in an autoclave, these tests were run in stroke-control. The stroke values in the autoclave tests were selected to match those measured in the corresponding strain-control test in air. Rather than match the stroke values in the two tests on a cycle-by-cycle basis, average values over a range of cycles were selected, as shown in Fig. 5. Benchmark tests were performed to show that the lives obtained under the variable amplitude stroke control were consistent with those obtained under strain control. These results are summarized in Table 6. Variations in life between the strain- and stroke-control tests are small and are within the scatter expected for tests in strain control at this strain range.

The tests in the simulated BWR environment were performed in high-purity water at 288°C with ~200 ppb dissolved oxygen in the effluent water. The lives at a given strain range in the environment are dependent on frequency. The results of the tests to date are summarized in Table 7.

The normalized fatigue life N_{env}/N_{air} is relatively independent of strain range, at least over the strain ranges examined to date, and depends primarily on the strain rate as shown in Fig. 6. The data show that at the lowest strain rates, the life in the simulated BWR environment is about one third that in air. The data are too limited at this point to assess whether the strain-rate effect has reached saturation, i.e., whether further decreases in the strain rate would not lead to a corresponding decrease in fatigue life.

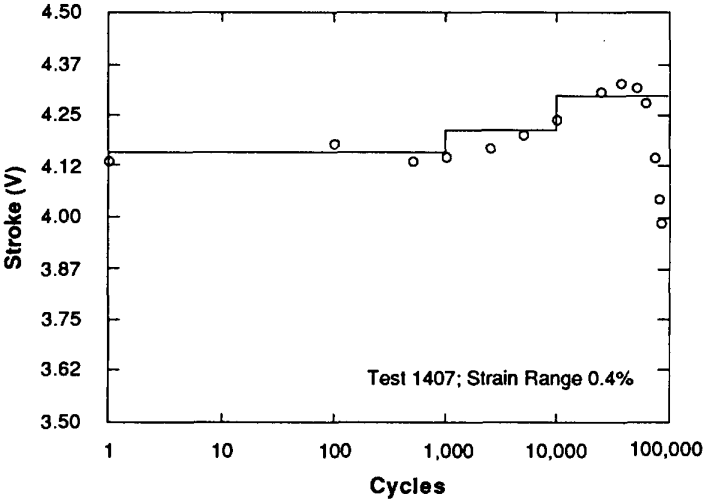

Figure 5.
Variable Amplitude Stroke History Used to Simulate Strain Control.

Table 6. Comparison of Fatigue Lives of Type 316NG SS in Strain and Stroke Control

Test No.	Control Type	Strain Range, %	Temp., °C	Cycles to Failure
1392	Strain	0.5	~22	60,741
1420	Stroke[a]	0.5	~22	54,249
1409	Strain	0.5	288	53,144
1410	Stroke	0.5	288	51,194

[a]Test performed with autoclave.

Table 7. Comparison of Fatigue Lives of Type 316NG SS in Air and Simulated BWR Water

Test No.	Environment	Strain Range, %	Frequency, Hz	Cycles to Failure
1409	Air[a]	0.5	0.5	53,194
1410	Air[b]	0.5	0.5	51,194
1420	Air[c]	0.5	0.5	54,249
1414	Water[d]	0.5	0.5	26,230
1418	Water[d]	0.5	0.5	25,714
1423	Water[d]	0.5	0.05	17,812
1425	Water[d]	0.5	0.005	13,684
1408	Air[a]	0.75	0.33	21,548
1426	Water[d]	0.75	0.5	12,069
1427	Water[d]	0.75	0.05	6,679
1428	Water[d]	0.75	0.005	5,897
1430	Air[a]	0.30	0.33	168,852
1431	Water[d]	0.30	0.5	116,754
1434	Water [4]	0.30	0.05	40,643

[a] Baseline test in air at 288°C under strain control.
[b] Baseline test in air at 288°C under stroke control.
[c] Baseline test in air at ~22°C under stroke control in the autoclave.
[d] High-purity water with 0.2 ppm dissolved oxygen at 288°C.

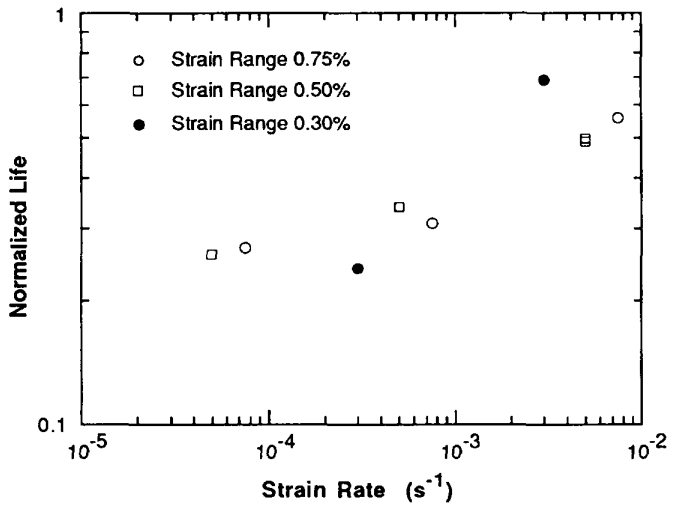

Figure 6.
Normalized Fatigue Life of Type 316NG SS in Simulated BWR Water at 288°C as a Function of Strain Rate.

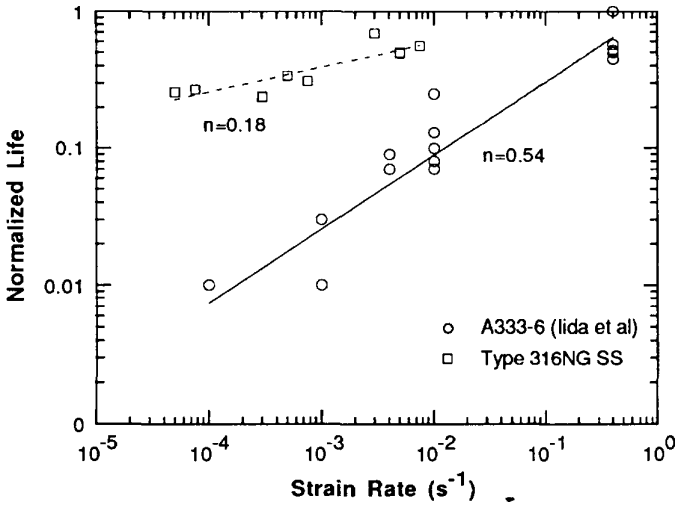

Figure 7.
Comparison of the Effect of Strain Rate on Normalized Fatigue Life of A333-Gr 6 Steel and Type 316NG SS.

These results may be compared with similar data obtained by Iida et al.[15] for an A333-Gr 6 steel in water with 8 ppm dissolved oxygen as shown in Fig. 7. The A333 steel shows a stronger strain rate dependence and a more severe reduction in fatigue life. In this case, the relative fatigue life is also almost independent of strain range for values from ~0.2 to 1%.

3 Influence of Water Chemistry on SCC of Type 304 SS

The objective of this part of the work is to evaluate the potential effectiveness of proposed actions to solve or mitigate the problem of IGSCC in BWR systems through modifications of water chemistry. In this regard, the effects of dissolved oxygen (produced by radiolytic decomposition of the water), anion impurities (e.g., oxyacids from decomposition of ion exchange resins during intrusions into the primary system), and several corrosion-product cations on the IGSCC susceptibility and crack growth properties of austenitic

stainless steels have been evaluated. The potential benefits associated with small additions of hydrogen to the coolant were also evaluated under conditions in which ionic impurities (e.g., oxyanions) were present at low concentrations in the high-temperature water.

The results of our tests suggest that the crack growth rate of the sensitized steel at strain rates in the regime where SCC occurs is limited by the rate of cathodic reduction of dissolved oxygen, various oxyanion impurity species, and Cu^{2+} or Cu^{+} in the high-temperature water. The amount of incremental crack advance per film rupture event at the crack tip is determined by the stoichiometry and kinetics of the individual cathodic reactions, although crack growth rates increase with crack-tip strain rate because the frequency of film rupture increases. At very high impurity levels, which are outside the range of simulated BWR water chemistry, crack growth rates become independent of impurity concentration and are limited solely by the strain rate, i.e., the frequency of film rupture. This interrelationship between mechanical loading conditions (applied or crack-tip strain rate) and water chemistry (concentration of dissolved oxygen, oxyanions, and Cu^{+}) provides the rationale for SCC remedies based upon lower residual and operating stresses (including cyclic loads) and lower impurity levels coupled with hydrogen additions to the water to suppress radiolysis of the coolant.

Certain organic impurities that adsorb on the corrosion product surface and block active sites for oxygen reduction have been found to mitigate IGSCC of the steel in fracture mechanics tests. The crack growth behavior of the steels was correlated with the type and concentration of impurities in the water, as well as with the open-circuit corrosion potential of the steel and platinum.

3.1 Technical Progress

3.1.1 Effect of Chromate in Water with ~5 and 200 ppb Dissolved Oxygen on SCC (W. E. Ruther, W. K. Soppet, and T. F. Kassner)

Soluble corrosion products from system materials are the major species present in the BWR water when ingress of ionic impurities into the coolant system from leaks in condenser tubes and from the ion-exchange resins in the reactor water cleanup system, including resin fines, is maintained at very low levels. Examples include Cu^{+} and Cu^{2+} in plants with either copper alloy condenser tubes and/or feedwater heaters and $HCrO_4^{-}$ from corrosion of stainless steel piping, weld cladding on the interior of the reactor vessel, and internal components fabricated from this material. Although chromate (K_2CrO_4) is used as a corrosion inhibitor in component cooling water systems (CCWS) in BWRs and PWRs,[16] these systems operate at relatively low temperatures (~170°C) and pressures (~150 psig), and direct ingress of chromate from the CCWS into the reactor coolant water is unlikely under normal operating conditions. Nevertheless, because only a small fraction (3–6%) of the recirculation water in BWRs passes through the RWCS, the concentration of corrosion-product ions in the reactor water can be considerably greater than in the feedwater (e.g., ~30–40 ppb versus <1 ppb, respectively). The effect of copper ions on SCC of sensitized Type 304 SS in low-oxygen (<5 ppb) water has been reported.[17,18]

The effect of chromate on SCC of the steel was investigated by CERTs in water with ~200 and <5 ppb dissolved oxygen. Chromate was added to the feedwater as either H_2CrO_4 or K_2CrO_4 over the concentration range of ~0.05 to 90 ppm. Analogous to our previous

results on the effect of dissolved oxygen and various oxyanions on SCC of the steel,[19,20] if cathodic reduction of the chromate ion to chromite or Cr_2O_3 is the rate controlling step in the overall SCC process and occurs according to the reactions

$$CrO_4^{2-} + 2H_2O + 3e^- = CrO_2^- + 4OH^- \quad (1)$$

$$HCrO_4^- + H_2O + 3e^- = CrO_2^- + 3OH^- \quad (2)$$

$$2HCrO_4^- + 3H_2O + 6e^- = Cr_2O_3 + 8OH^-, \quad (3)$$

the corresponding chemical equilibria can be written as

$$K_{eq} = [OH^-]^4 [CrO_2^-] / [e^-]^3 [CrO_4^{2-}] \quad (4)$$

$$K_{eq} = [OH^-]^3 [CrO_2^-] / [e^-]^3 [HCrO_4^-] \quad (5)$$

$$K_{eq} = [OH^-]^8 [Cr_2O_3] / [e^-]^6 [HCrO_4^-]^2, \quad (6)$$

and the reciprocal of the electron concentration would depend on the concentration of chromate as given by

$$1/[e^-] = k_1 [CrO_4^{2-}]^{1/3} / [OH^-]^{4/3} [CrO_2^-]^{1/3} \quad (7)$$

$$1/[e^-] = k_2 [HCrO_4^-]^{1/3} / [OH^-] [CrO_2^-]^{1/3} \quad (8)$$

$$1/[e^-] = k_3 [HCrO_4^-]^{1/3} / [OH^-]^{4/3} [Cr_2O_3]^{1/6}. \quad (9)$$

Because the CGR is proportional to $1/[e^-]$ for many impurity species that undergo cathodic reduction,[17-20] Eqs. (7)–(9) indicate that the CGR should depend on the 1/3–power of the chromate concentration in low–oxygen water for the electrochemical potential–pH regime corresponding to Eqs. (1)–(3), if cathodic reduction of the chromate ion is the rate–controlling step.

The experimental results in Table 8 and Fig. 8 indicate that the CGRs indeed exhibit this dependence over a wide range of chromate concentration and conductivity of the feedwater, irrespective of the $pH_{25°C}$. Although $pH_{25°C}$ or $pH_{289°C}$ in itself is not an important factor in SCC under these conditions, the dependence of the CGR on $pH_{25°C}$ in Fig. 9 is consistent with the relationship between the chromate concentration and $pH_{25°C}$ for both acidic and basic solutions.

The dependence of electrochemical potential (ECP) of the steel and the platinum electrode on chromate concentration and conductivity of the feedwater in the CERTs is shown in Figs. 10 and 11. The ECP values for Type 304 SS in acidic solutions (H_2CrO_4) increase from ~–350 to +500 mV(SHE) over the concentration range of ~0.1 to 50 ppm chromate. In near–neutral and basic solutions (K_2CrO_4), the ECP values increase from ~–350 to ~0 mV (SHE) over the range of ~0.03 to 0.3 ppm and then decrease to <–100 mV (SHE) as the chromate concentration increases to 90 ppm. The ECP values of the platinum electrode follow similar trends. As indicated by the filled symbols in Fig. 9, IGSCC occurs at ECP values >–100 mV (SHE), whereas TGSCC is observed at lower values. The dependence of the CGR on the 1/3–power of the chromate concentration and conductivity in Fig. 8 is primarily applicable to the IGSCC regime, because the CGRs for TGSCC, which occurred at

Table 8. Influence of H_2CrO_4 and K_2CrO_4 at Low Dissolved-Oxygen Concentration (<5 ppb) on the SCC Susceptibility of Sensitized Type 304 SS Specimens[a] in 289°C Water

	Feedwater Chemistry			CERT Parameters						Potential	
Test No.	Anion Conc., ppm	Cond. at 25°C, $\mu S \cdot cm^{-1}$	pH at 25°C	Failure Time, h	Maximum Stress, MPa	Total Elong., %	Reduction in Area, %	SCC Growth Rate,[b] $m \cdot s^{-1}$	Fracture Morphology[c]	304 SS, mv(SHE)	Pt, mv(SHE)
A170	0.1	0.50	5.93	123	509	44	49	4.3×10^{-9}	0.42D, 0.58T	-540	-498
A187	0.2	0.83	5.85	97	497	35	42	4.7×10^{-9}	0.65D, 0.35G_3	12	31
A186	0.3	1.08	5.74	98	480	35	41	6.2×10^{-9}	0.57D, 0.43G_3	9	-5
A171	1.0	3.50	5.17	77	423	28	40	7.2×10^{-9}	0.39D, 0.61G_3	80	86
A174	5.0	18.1	4.43	56	366	20	34	1.4×10^{-8}	0.20D, 0.80I	284	278
A172	10.0	34.0	4.14	54	358	20	28	2.0×10^{-8}	0.14D, 0.86I	341	337
A173	50.0	175.0	3.42	44	367	16	22	2.0×10^{-8}	0.30D, 0.70I	487	483
A177[d]	0.05	0.35	6.71	128	513	46	49	2.2×10^{-9}	0.68D, 0.32T	-333	-312
A188[d]	0.1	0.46	6.33	140	519	50	52	1.1×10^{-9}	0.81D, 0.19T	-167	-191
A176[d]	0.5	1.46	7.07	100	487	36	52	8.0×10^{-9}	0.39D, 0.61G_3	-9	-16
A179[d]	1.0	2.56	7.48	95	479	34	52	1.0×10^{-8}	0.22D, 0.78G_3	-1	-10
A175[d]	5.0	14.1	7.44	72	426	26	38	1.1×10^{-8}	0.52D, 0.48I	-25	-23
A178[d]	90.0	230.0	8.54	56	376	20	32	2.9×10^{-8}	0.05D, 0.95I	-140	-138

[a] Lightly sensitized (EPR = 2 $C \cdot cm^{-2}$) specimens (Heat No. 30956) were exposed to the environments for ~20 h before being strained at a rate of 1×10^{-6} s^{-1}.

[b] SCC growth rates are based on measurement of the depth of the longest crack in an enlarged micrograph of the fracture surface and the time period from the onset of yield to the point of maximum load on the tensile curve.

[c] Ductile (D), transgranular (T), granulated (G), and intergranular (I), in terms of the fraction of the cross-sectional area. Characterization of the fracture surface morphologies is in accordance with the illustrations and definitions in Reference 21.

[d] Chromate added as K_2CrO_4.

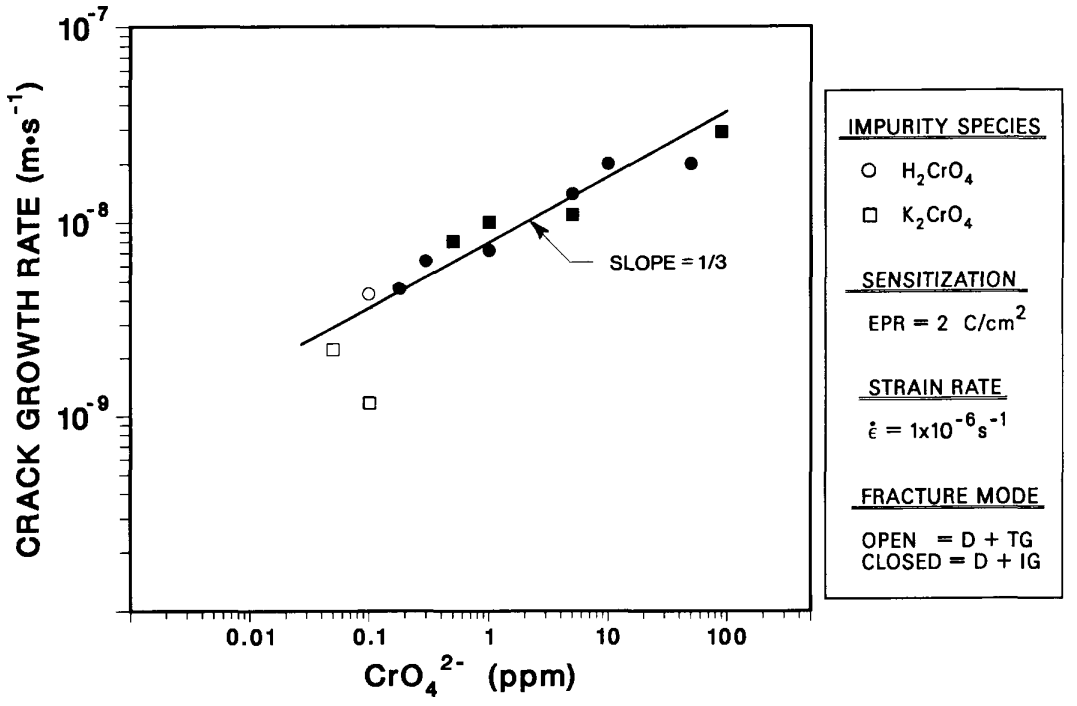

(a)

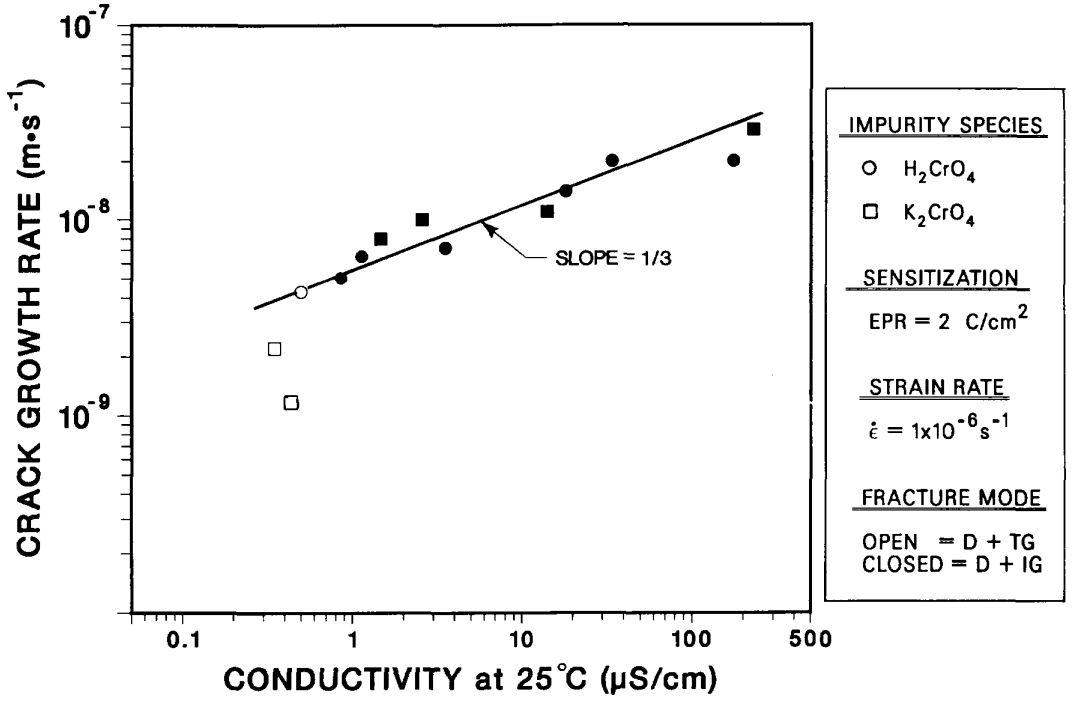

(b)

Figure 8. Dependence of the CGR of Sensitized Type 304 SS CERT Specimens at 289°C on (a) Concentration of Chromate and (b) Conductivity of the Low-Oxygen (<5 ppb) Feedwater. Open and closed symbols denote ductile plus transgranular and ductile plus intergranular fracture morphologies, respectively.

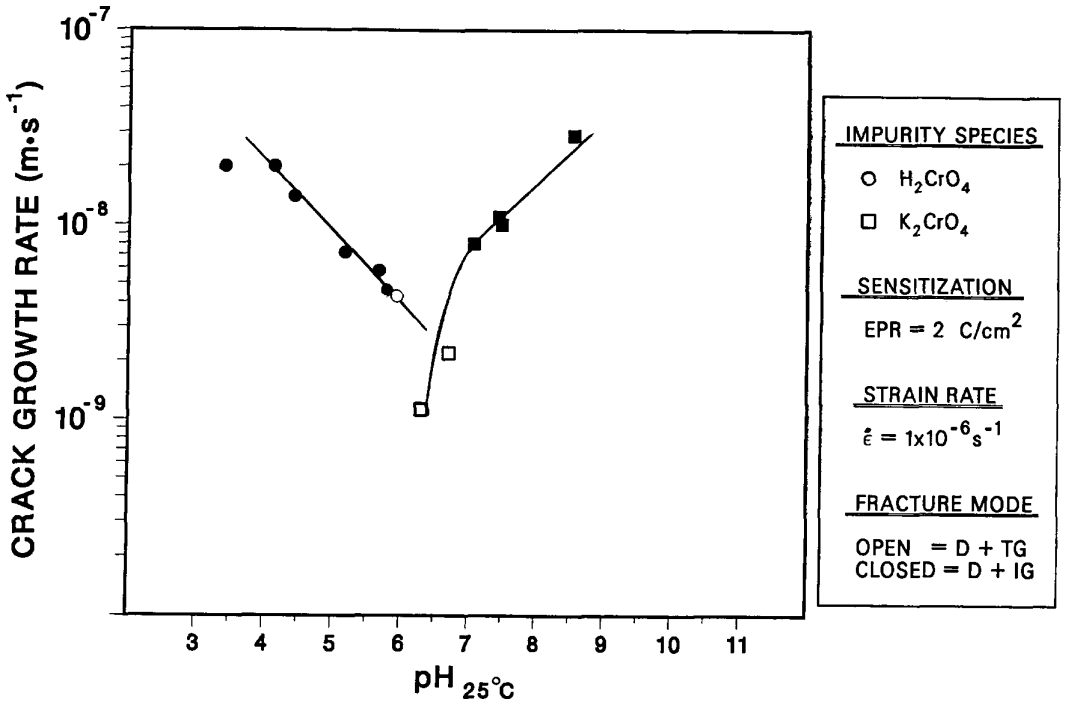

Figure 9. Dependence of the CGR of Sensitized Type 304 SS CERT Specimens at 289°C on $pH_{25°C}$ of the Low-Oxygen (<5 ppb) Feedwater. Open and closed symbols denote ductile plus transgranular and ductile plus intergranular fracture morphologies, respectively.

low chromate concentrations (<0.1 ppm) and ECP values (< −150 mV [SHE]), tend to fall below the trend line.

The effect of chromate in water containing ~200 ppb dissolved oxygen on the SCC behavior of sensitized Type 304 SS was also investigated. The results, which are given in Table 9 and Fig. 12, indicate that chromate additions to the oxygenated water increase the CGRs. However, the dependence on concentration is weaker at the higher oxygen level. For example, the CGR in oxygenated water with 100 ppb chromate is higher by a factor of ~2.5 than in low-oxygen water at the same chromate concentration, but the CGRs are the same (~1.0 x 10^{-8} m·s^{-1}) in the high- and low-oxygen environments at chromate concentration of ~1.0 ppm. In comparison with other species at the 100 ppb level in simulated BWR water (~200 ppb dissolved oxygen),[22] chromate is less deleterious than sulfate and arsenate, and more deleterious than nitrate, borate, carbonate, and chloride in CERT tests at 289°C and a strain rate of 1 x 10^{-6} s^{-1}.

The effect of chromate on the ECP of Type 304 SS and platinum in oxygenated water is shown in Figs. 13 and 14. When chromate is present in acid form, the ECP values of the steel and platinum increase from ~50 mV(SHE) at a concentration of ~0.1 ppm to +350 mV(SHE) at the 10 ppm level. When chromate is added to the feedwater as K_2CrO_4, the ECP values of Type 304 SS decrease from ~50 to −100 mV(SHE) over this concentration range, but the values for platinum are not dependent on the chromate concentration.

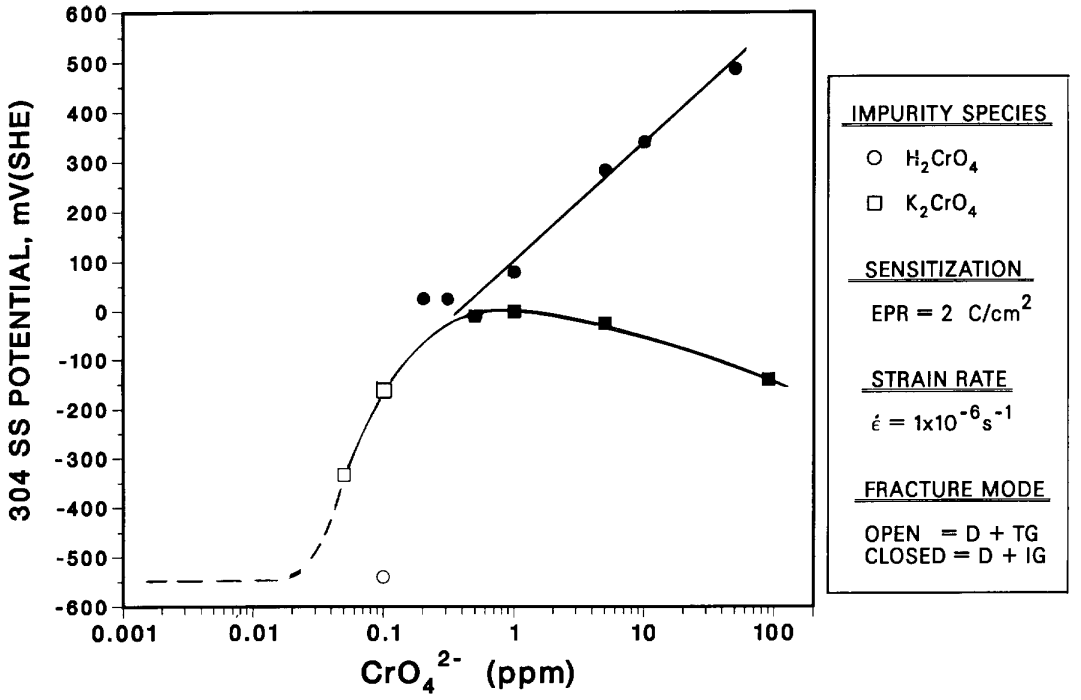

(a)

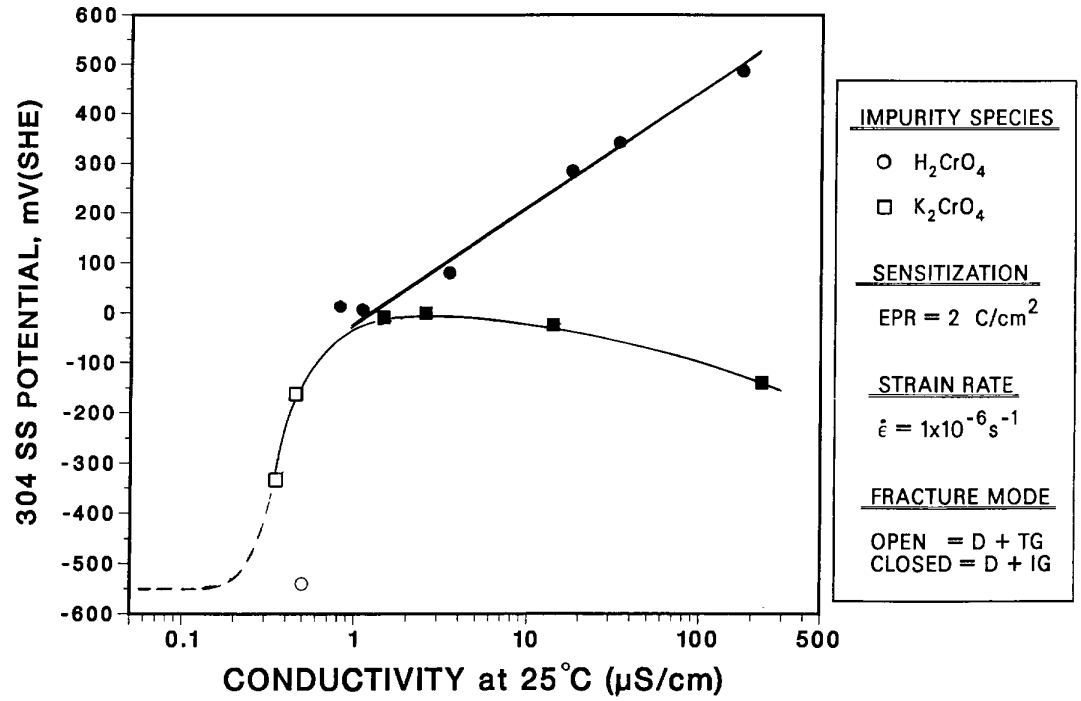

(b)

Figure 10. Dependence of the Steady-State Electrochemical Potential of Type 304 SS on (a) Concentration of Chromate and (b) Conductivity of the Low-Oxygen (<5 ppb) Feedwater during CERTs on Sensitized Type 304 SS Specimens at 289°C. Open and closed symbols denote ductile plus transgranular and ductile plus intergranular fracture morphologies, respectively.

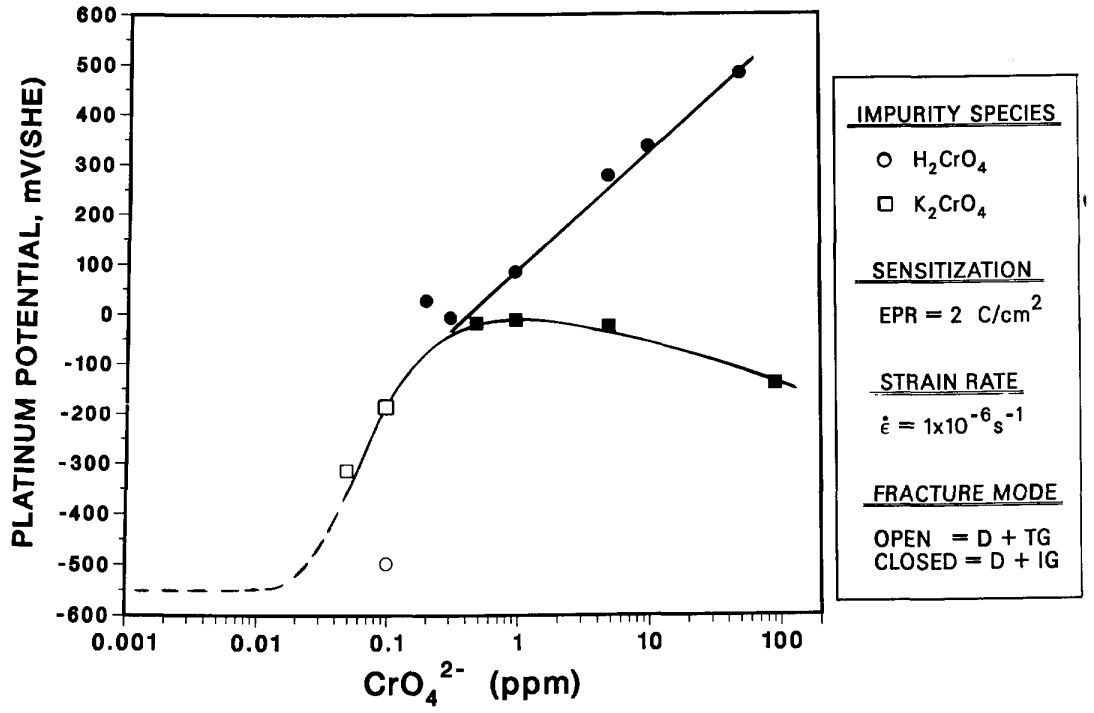

(a)

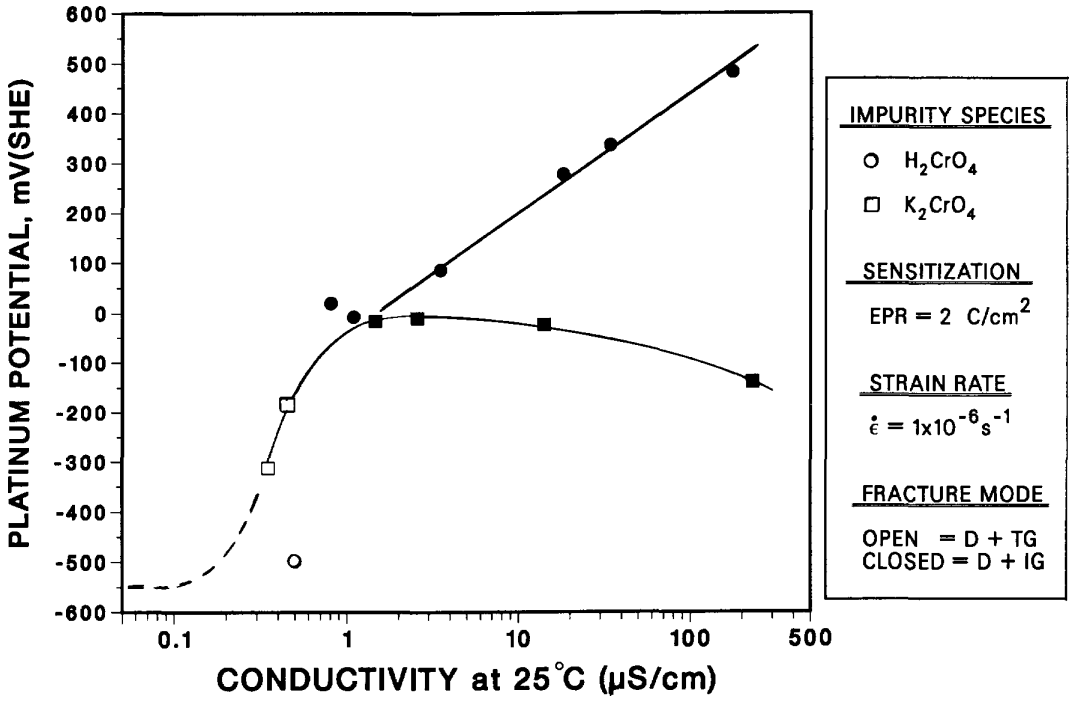

(b)

Figure 11. Dependence of the Steady-State Electrochemical Potential of Platinum on (a) Concentration of Chromate and (b) Conductivity of the Low-Oxygen (<5 ppb) Feedwater during CERTs on Sensitized Type 304 SS Specimens at 289°C. Open and closed symbols denote ductile plus transgranular and ductile plus intergranular fracture morphologies, respectively.

Table 9. Influence of H_2CrO_4 and K_2CrO_4 on the SCC Susceptibility of Sensitized Type 304 SS Specimens[a] in Water Containing ~200 ppb Dissolved Oxygen at 289°C

	Feedwater Chemistry				CERT Parameters						Potentials	
Test No.	Oxygen, ppb	Anion Conc., ppm	Cond. at 25°C, $\mu S \cdot cm^{-1}$	pH at 25°C	Failure Time, h	Maximum Stress, MPa	Total Elong., %	Reduction in Area, %	SCC Growth Rate,[b] $m \cdot s^{-1}$	Fracture Morphology[c]	304 SS, mv(SHE)	Pt, mv(SHE)
A2	240	–	0.14	6.12	166	493	60	66	4.0×10^{-9}	0.80D, 0.20T	44	60
A183	230	0.1	0.61	6.02	76	442	27	40	6.5×10^{-9}	0.66D, 0.34G_3	54	66
A184	230	1.0	3.40	5.17	72	422	26	36	9.1×10^{-9}	0.41D, 0.59I	155	173
A185	220	10.0	34.0	4.14	47	337	17	30	1.8×10^{-8}	0.12D, 0.88I	348	337
A180[d]	220	0.1	0.48	6.68	95	479	34	43	6.8×10^{-9}	0.49D, 0.51I	50	59
A181[d]	240	1.0	2.70	7.02	82	442	29	41	9.8×10^{-9}	0.53D, 0.47G_3	6	27
A182[d]	250	5.0	9.80	7.75	75	411	27	51	9.4×10^{-9}	0.38D, 0.62I	-30	52

[a] Lightly sensitized (EPR = 2 $C \cdot cm^{-2}$) specimens (Heat No. 30956) were exposed to the environments for ~20 h before being strained at a rate of 1×10^{-6} s^{-1}.

[b] SCC growth rates are based on measurement of the depth of the longest crack in an enlarged micrograph of the fracture surface and the time period from the onset of yield to the point of maximum load on the tensile curve.

[c] Ductile (D), transgranular (T), granulated (G), and intergranular (I), in terms of the fraction of the cross-sectional area. Characterization of the fracture surface morphologies is in accordance with the illustrations and definitions in Reference 21.

[d] Chromate added as K_2CrO_4.

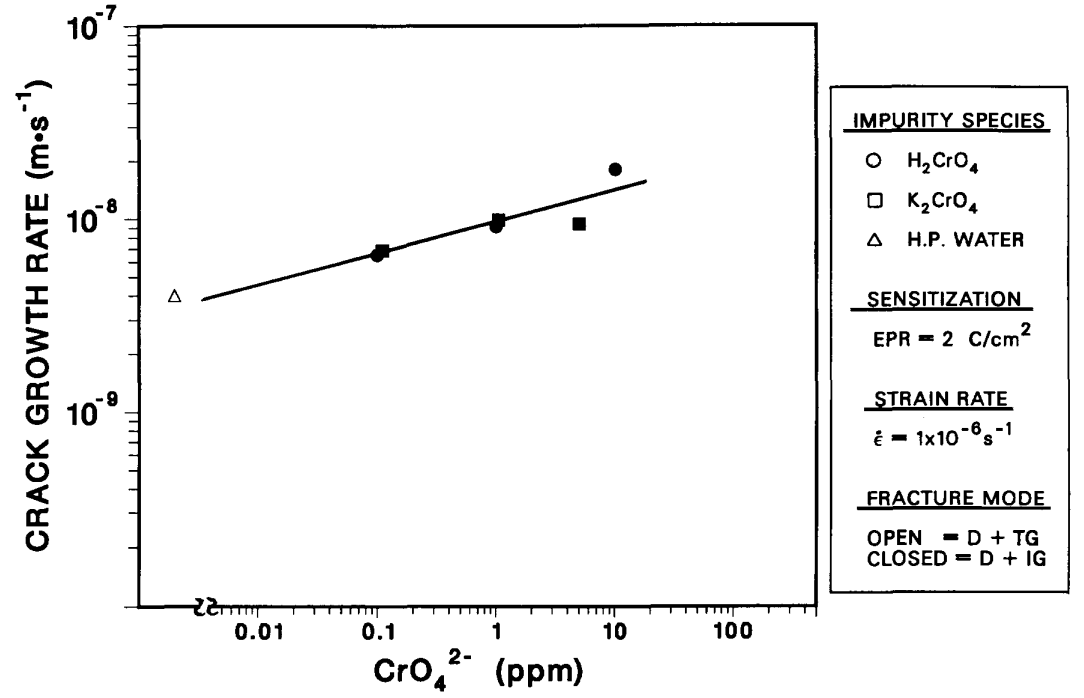

(a)

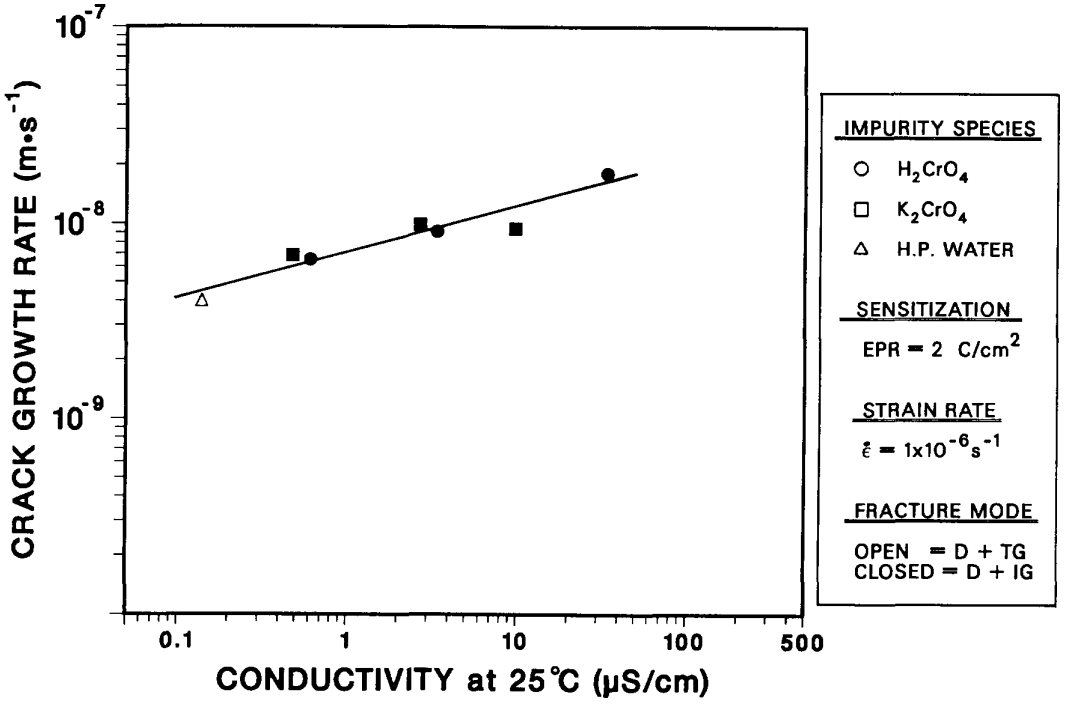

(b)

Figure 12. Dependence of the CGR of Sensitized Type 304 SS CERT Specimens at 289°C on (a) Concentration of Chromate and (b) Conductivity of the Oxygenated (~200 ppb) Feedwater. Open and closed symbols denote ductile plus transgranular and ductile plus intergranular fracture morphologies, respectively.

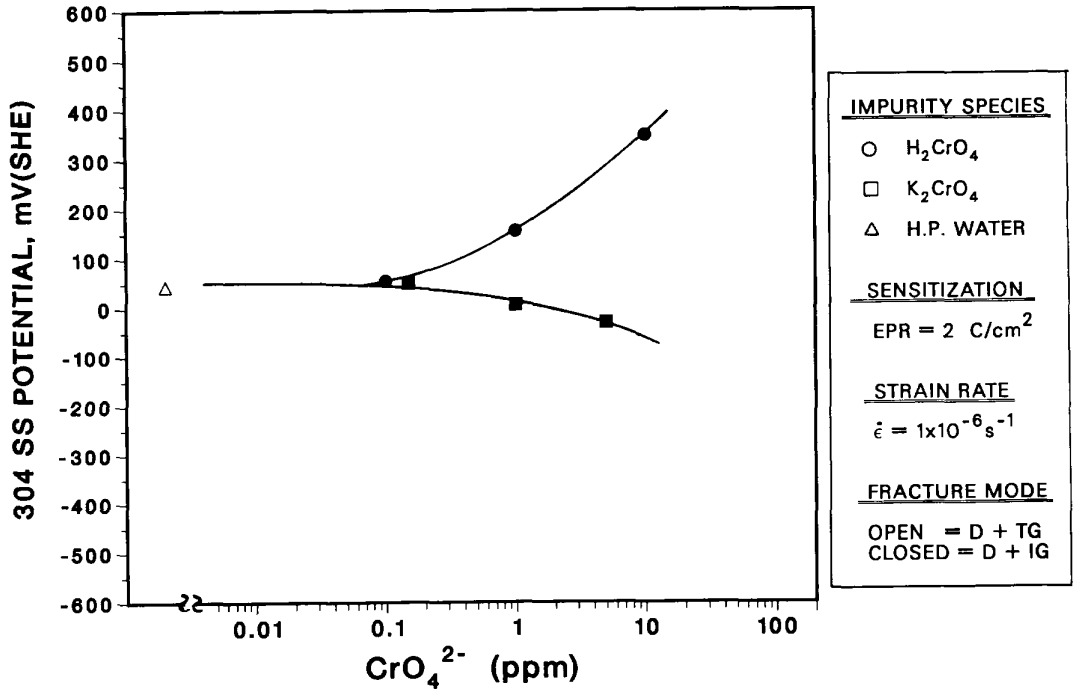

(a)

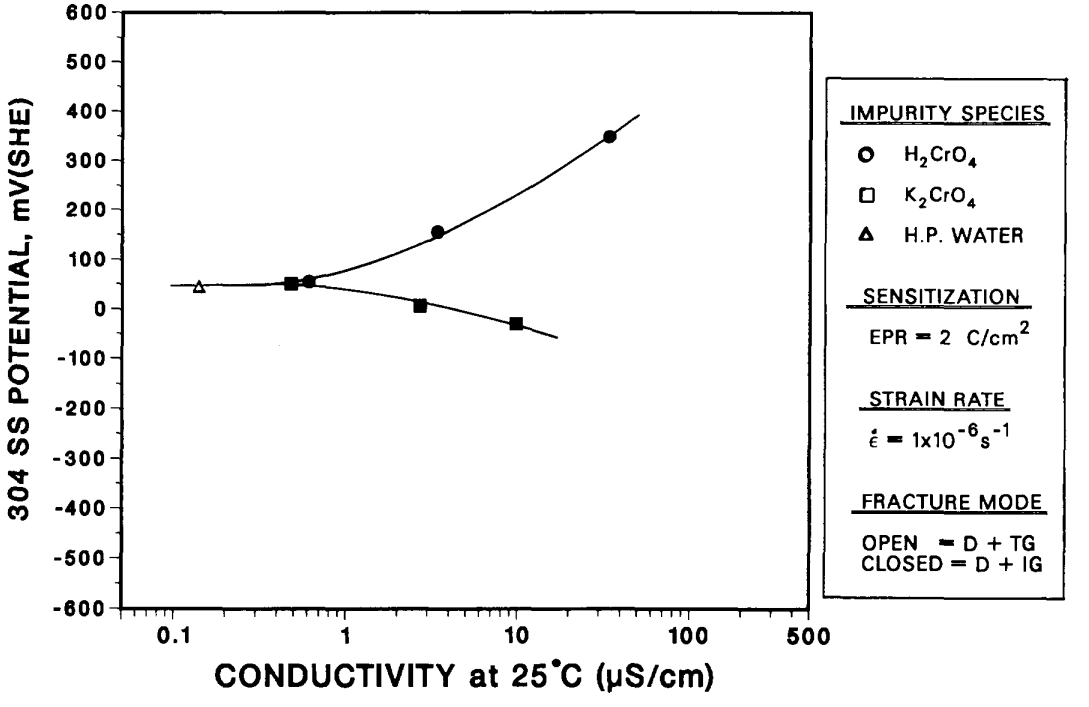

(b)

Figure 13. Dependence of the Steady-State Electrochemical Potential of Type 304 SS on (a) Concentration of Chromate and (b) Conductivity of the Oxygenated (~200 ppb) Feedwater during CERTs on Sensitized Type 304 SS Specimens at 289°C. Open and closed symbols denote ductile plus transgranular and ductile plus intergranular fracture morphologies, respectively.

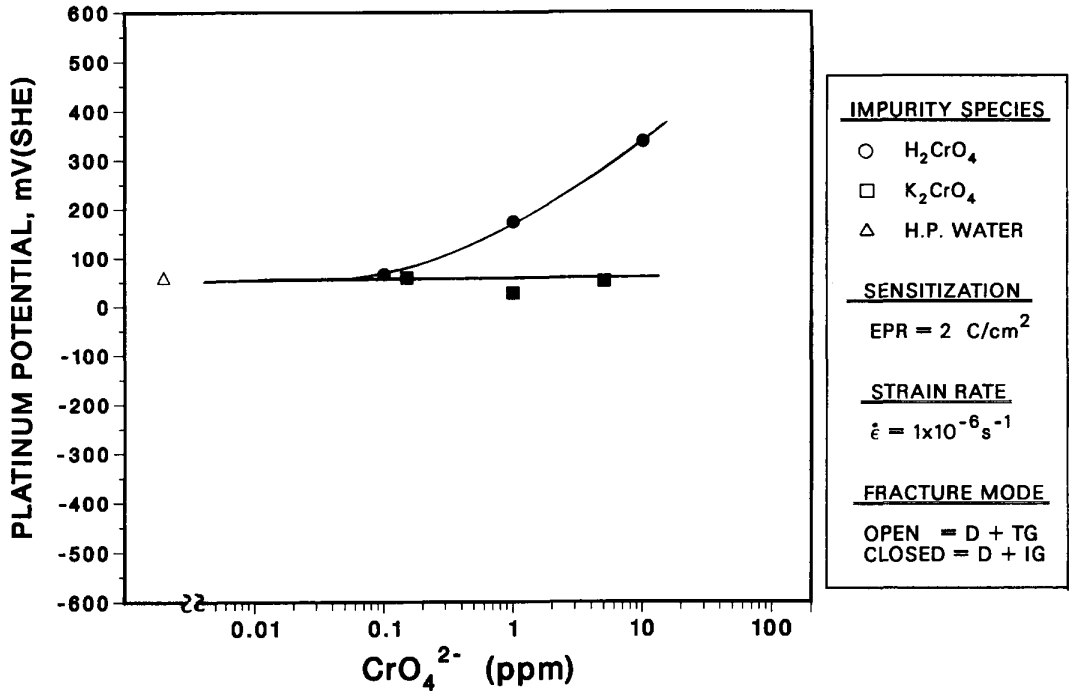

(a)

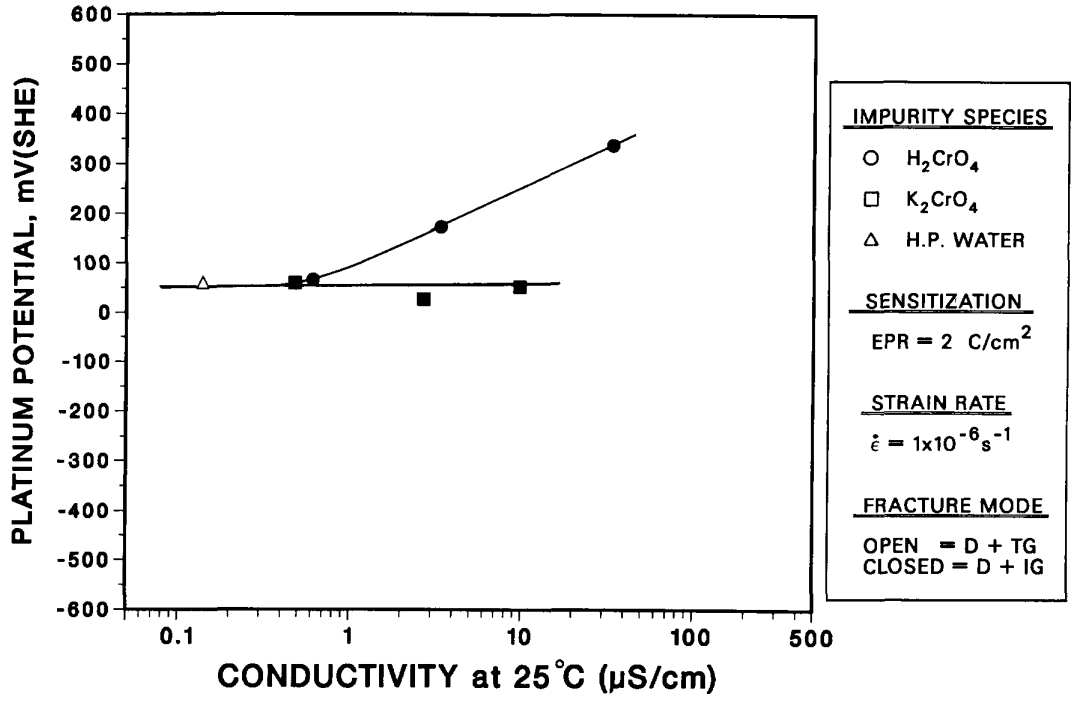

(b)

Figure 14. Dependence of the Steady-State Electrochemical Potential of Platinum on (a) Concentration of Chromate and (b) Conductivity of the Oxygenated (~200 ppb) Feedwater during CERTs on Sensitized Type 304 SS Specimens at 289°C. Open and closed symbols denote ductile plus transgranular and ductile plus intergranular fracture morphologies, respectively.

The CERT results indicate that chromate acts in a similar manner to other oxyanions in its effect on SCC of sensitized Type 304 SS. These species undergo cathodic reduction and contribute to crack growth by scavenging electrons produced by anodic dissolution of metal at the crack tip in a slip–dissolution mechanism[23,24] of crack advance. IGSCC occurs at chromate concentrations >0.1 ppm in the absence or presence of dissolved oxygen; however, the rates are somewhat higher in the latter environment because both oxygen and chromate undergo cathodic reduction and contribute to the overall cathodic partial process.

3.1.2 Effect of Organic Substances in Oxygenated Water on SCC at 289°C (W. E. Ruther, W. K. Soppet, and T. F. Kassner)

Typical chemicals at power plants include paint products, glycol, hydraulic fluids, lubricants, detergents, chemical cleaners, laundry chemicals, freons, diesel fuel, and ion-exchange resin regeneration chemicals. Potential chemical contaminants[25] and possible pathways[26] for entry of various substances into BWR coolant systems have been evaluated. Some of the long-lived products that may exist in BWR water due to organic intrusions are carboxylic acids, alcohols, phenolics, aromatic hydrocarbons, hydrogen halides, sulfuric and sulfonic acids, amines, and other substances.[25] These organic impurities and their decomposition products are a potential concern in BWR water and PWR secondary-system water in terms of increased susceptibility to localized corrosion and SCC of piping and heat-exchanger tube materials.

Organic impurities are also a concern in PWR secondary-coolant water systems because organic acids increase cation conductivity, which complicates secondary water monitoring and control. A recent survey of organic acids, total organic carbon, and inorganic anions in the secondary water cycles of 13 PWRs indicated that organic acids were responsible for a major fraction of the cation conductivity in many of the plants.[27] Acetic and formic were the most common acids; however, lactic, propionic, and butyric acids were also present in some of the systems. Make-up water was the major source of the organic impurities, some of which were in colloidal, nonionic form.[27]

To distinguish between the role of organic oxygen scavengers, which react with dissolved oxygen in the water, and that of other organic species, which conceivably adsorb on the material surface and influence cathodic reduction of oxygen, the effect of both types of organic substances on SCC susceptibility of sensitized Type 304 SS was investigated. Subsequently, the influence of several carboxylic acids on the SCC behavior of the steel was determined in cyclic loading tests on fracture-mechanics-type specimens in oxygenated water.

The organic substances that were investigated are listed in Table 10. The oxygen scavengers are commonly used to control corrosion of carbon-steel boiler and copper-alloy condenser tubing in fossil-fired steam-generating systems,[28] whereas the organic acids are among those species found in BWR and PWR coolant systems at low concentrations due to ingress and decomposition of organic substances used in the plants. Although chemical oxygen scavengers are not typically used in reactor coolant systems (in contrast to hydrazine and hydrogen, which are added to the feedwater in PWR steam generators[29] and in BWRs,[30] respectively), their beneficial effect can be rationalized in terms of the well-known influence of low-oxygen concentration on the ECP and SCC susceptibility of

Table 10. Organic Substances Used in SCC Tests on Sensitized Type 304 SS

Substance	Formula
Oxygen Scavengers	
Ascorbic acid	$C_6H_8O_6$
Hydroquinone	$C_6H_4(OH)_2$
Carbohydrazide	$(N_2H_3)_2CO$
2-Butanoneoxime	$CH_3CH_2C(=NOH)CH_3$
N,N Diethylhydroxylamine	$(C_2H_5)_2NOH$
Organic Acids	
Formic	$HCOOH$
Acetic	CH_3COOH
Lactic	$CH_3CH(OH)COOH$
Oxalic	$(COOH)_2$
Propionic	CH_3CH_2COOH
Butyric	$CH_3(CH_2)_2COOH$
Valeric	$CH_3(CH_2)_3COOH$
Benzoic	C_6H_5COOH
Carbonic	H_2CO_3

austenitic stainless steels.[17-20, 31-33] Although the organic acids could act in a similar manner, i.e., scavenge oxygen, other mechanisms can, in principle, account for their effect on SCC of sensitized Type 304 SS in high-temperature water.

The data in Table 11 summarize the influence of several chemical oxygen scavengers at a concentration of 1.0 ppm in feedwater containing 200 ppb dissolved oxygen on the CERT parameters of lightly sensitized Type 304 SS at 289°C. Failure times increase and the crack growth rates decrease markedly when these species are added to the feedwater. The low effluent values (<10 ppb) and the large decrease in the ECP values for Type 304 SS and the platinum electrode (i.e., to <-180 mV[SHE] from ~+90 and ~+180 mV, respectively) demonstrate that these species react with dissolved oxygen in the water. In the cases of N,N diethylhydroxylamine and 2-butanoneoxime, which have minimal effects on feedwater conductivity and pH, the fracture mode was 100% ductile and the time-to-failure increased by a factor of 3 compared to that in high-purity water. These two species were particularly effective in mitigating SCC.

The effects of several carboxylic acids (acetic, formic, lactic, oxalic, propionic, butyric, and valeric) at a concentration of 1.0 ppm on the SCC susceptibility of sensitized Type 304 SS in oxygenated water are shown in Table 12. In contrast to the previous results, these species increase the time-to-failure by at most a factor of ~2, and with a few exceptions, the ECP of the steel decreases by ~30 mV relative to that in high-purity water. For the

Table 11. Influence of Several Organic Oxygen Scavengers on the SCC Susceptibility of Sensitized Type 304 SS Specimens[a] in 289°C Water at a Feedwater Dissolved-Oxygen Concentration of ~200 ppb

	Feedwater Chemistry					CERT Parameters						Potential	
Test No.	O_2 Conc., ppb	Organic O_2 Scavenger	Conc., ppm	Cond., $\mu S \cdot cm^{-1}$	pH at 25°C	Failure Time, h	Maximum Stress, MPa	Total Elong., %	Reduction in Area, %	Fracture Morphology[b]	SCC Growth Rate,[c] $m \cdot s^{-1}$	304 SS, mV(SHE)	Pt, mV(SHE)
A144	250	-	-	0.26	6.43	73	297	14	15	0.16D, 0.84I	1.5×10^{-8}	98	158
A143	180	-	-	0.16	6.21	101	350	19	12	0.16D, 0.84I	9.6×10^{-9}	86	196
A196	240	l-Ascorbic	1.0	1.8	5.44	237	523	44	31	0.49D, 0.51T	1.3×10^{-9}	-578[d]	-497[d]
A198	200	iso-Ascorbic	1.0	1.8	5.29	210	-	39	28	0.42D, 0.58G_3	2.1×10^{-9}	-184[d]	-395[d]
A197	220	Hydroquinone	1.0	0.11	6.23	272	527	51	46	0.36D, 0.64G_3	1.1×10^{-9}	-395[d]	-275[d]
A199	230	Carbohydrazide	1.0	0.34	6.54	219	494	45	31	0.59D, 0.41T	1.6×10^{-9}	-607[d]	-531[d]
A200	250	2-Butanoneoxime	1.0	0.09	6.57	304	531	57	70	1.00D	0	-188[d]	-192[d]
A201	250	N,N Diethyl-hydroxylamine	1.0	0.12	6.53	305	525	57	73	1.00D	0	-359[d]	-361[d]

[a] Lightly sensitized (EPR = 2 $C \cdot cm^{-2}$) specimens (Heat No. 30956) were exposed to the environments for ~20 h before straining at a rate of 5.2×10^{-7} s^{-1}.

[b] Ductile (D), transgranular (T), granulated (G), and intergranular (I), in terms of the fraction of the cross-sectional area. Characterization of the fracture surface morphologies is in accordance with the illustrations and definitions in Reference 21.

[c] SCC growth rates are based on measurement of the depth of the longest crack in an enlarged micrograph of the fracture surface and the time period from the onset of yield to the point of maximum load on the tensile curve.

[d] Effluent dissolved oxygen concentration was <10 ppb by CHEMetrics colorimetric analyses.

Table 12. Influence of Several Organic Acids on the SCC Susceptibility of Sensitized Type 304 SS Specimens[a] in 289°C Water at a Feedwater Dissolved-Oxygen Concentration of ~200 ppb

	Feedwater Chemistry					CERT Parameters						Potential	
Test No.	O_2 Conc., ppb	Organic O_2 Scavenger	Conc., ppm	Cond., $\mu S \cdot cm^{-1}$	pH at 25°C	Failure Time, h	Maximum Stress, MPa	Total Elong., %	Reduction in Area, %	Fracture Morphology[b]	SCC Growth Rate,[c] $m \cdot s^{-1}$	304 SS, mV(SHE)	Pt, mV(SHE)
A144	250	-	-	0.26	6.43	73	297	14	15	0.16D, 0.84I	1.5×10^{-8}	98	158
A143	180	-	-	0.16	6.21	101	350	19	12	0.16D, 0.84I	9.6×10^{-9}	86	196
A146	210	Acetic	1.0	3.9	5.07	104	390	19	26	0.29D, 0.71I	7.0×10^{-9}	103	111
A147	230	Formic	1.0	7.2	4.81	118	393	22	28	0.33D, 0.67I	6.4×10^{-9}	9	-333
A148	230	Lactic	1.0	3.7	5.09	161	442	30	36	0.18D, 0.82G_3	4.3×10^{-9}	-206	-406
A151	240	Oxalic	1.0	7.4	4.80	208	513	39	44	0.48D, 0.52G_2	3.5×10^{-9}	-2	-255
A149	250	Propionic	1.0	3.1	5.16	201	513	38	41	0.61D, 0.39T	2.9×10^{-9}	26	-134
A150	240	n-Butyric	1.0	2.7	5.27	189	485	35	59	0.83D, 0.17G_3	2.3×10^{-9}	55	-228
A190	250	n-Butyric	1.0	2.8	5.20	190	485	35	31	0.23D, 0.77G_3	2.7×10^{-9}	54	0
A191	260	iso-Butyric	1.0	2.8	5.21	147	450	28	39	0.50D, 0.50G_3	3.5×10^{-9}	53	-
A192	260	n-Valeric	1.0	2.5	5.27	163	469	31	37	0.43D, 0.57G_3	3.2×10^{-9}	36	-102
A193	250	iso-Valeric	1.0	2.7	5.27	167	452	31	60	0.62D, 0.38G_3	3.0×10^{-9}	61	-125
A194	220	Benzoic	1.0	2.7	5.22	185	482	35	60	0.29D, 0.71G_3	2.6×10^{-9}	49	-274
A195	240	Na Benzoate	1.0	0.75	6.57	162	467	30	47	0.28D, 0.72G_3	3.2×10^{-9}	-2	-313
A152	220	Carbonic	1.0	0.60	5.90	207	505	39	58	0.79D, 0.21G_3	2.0×10^{-9}	18	-165

[a] Lightly sensitized (EPR = 2 $C \cdot cm^{-2}$) specimens (Heat No. 30956) were exposed to the environments for ~20 h before straining at a rate of 5.2×10^{-7} s^{-1}.

[b] Ductile (D), transgranular (T), granulated (G), and intergranular (I), in terms of the fraction of the cross-sectional area. Characterization of the fracture surface morphologies is in accordance with the illustrations and definitions in Reference 21.

[c] SCC growth rates are based on measurement of the depth of the longest crack in an enlarged micrograph of the fracture surface and the time period from the onset of yield to the point of maximum load on the tensile curve.

most part, the ECP values of the platinum electrode decreased to values below ~–100 mV(SHE), although the effluent dissolved oxygen concentration was >150 ppb by colorimetric analyses. The fracture mode of the specimens was intergranular in all instances except in the test with 1.0 ppm propionic acid, where TGSCC occurred. Results from a test with 1.0 ppm of carbonic acid are also included in Table 12, since this species is a likely decomposition product of the various acids at high temperatures in reactor coolant systems where a gamma radiation field also may be present. Carbonic acid does not appear to have a deleterious effect on SCC.

Table 13 presents results from a series of fracture-mechanics crack growth tests on sensitized Type 304 SS in deionized water containing 0.2–0.3 ppm dissolved oxygen, in oxygenated water with 0.1 and 1.0 ppm propionic or butyric acid, and in water with 1.0 ppm butyric acid and either 100 ppb sulfate or chloride. The crack length as a function of time is plotted in Figs. 15 and 16 for 10 tests conducted over ~10,500 h. A baseline CGR of 2.9×10^{-10} m·s^{-1} was obtained in deionized water in Test No. 1. The addition of 0.1 ppm propionic acid in Test No. 2 had no effect on the CGR, as can be seen in Table 13 and Fig. 15; however, an increase in concentration to 1.0 ppm (Test No. 3) caused a decrease in the CGR by an order of magnitude. When propionic acid was no longer added to the feedwater (Test No. 4), the CGR returned to the initial baseline value.

In Test No. 5, 1.0 ppm butyric acid was added to the oxygenated feedwater and no crack growth was observed over a time interval of ~1150 h under low-frequency, high-R loading at a K_{max} value of ~34 MPa·m$^{1/2}$. A decrease in the butyric acid concentration from 1.0 to 0.1 ppm eventually caused the CGR to increase to a value of 1.9×10^{-10} m·s^{-1} after ~500 h. The lower concentration of the acid was not sufficient to inhibit crack growth, as was the case in Test No. 2 with 0.1 ppm propionic acid in the feedwater.

In Test No. 7, the butyric acid concentration in the oxygenated feedwater was increased to 1.0 ppm, and 100 ppb sulfate (as H_2SO_4) was also added. As can be seen in Table 13 and Fig. 16, the CGR increased significantly to a value of 7.4×10^{-10} m·s^{-1}. When sulfate was removed from the feedwater in Test No. 8, the CGR once again decreased to zero over a period of ~600 h. In Test No. 9, 100 ppb chloride (as NaCl) was added to the oxygenated feedwater containing 1.0 ppm butyric acid. The CGR of the steel increased to a value of ~1.5×10^{-10} m·s^{-1} over an interval of ~1150 h. In the last experiment (No. 10), chloride was not added to the feedwater and the CGR again decreased to zero, even at the relatively high stress intensity factor of ~40 MPa·m$^{1/2}$. The results in Tests 7–10 clearly indicate that the organic acid was not effective in inhibiting crack growth in the material when either sulfate or chloride was present in the oxygenated water at relatively low concentrations.

The ECP values of the Type 304 SS and the platinum electrode were monitored throughout the tests. The results in Table 13 indicate that the ECP of the Type 304 SS and platinum did not decrease when the organic acids were present in the water, in contrast to the CERT experiments in Table 12 where the ECP values of the platinum electrode were lower by ~400 mV than the values obtained in high-purity oxygenated water. This can be attributed to the higher oxygen concentrations in the feedwater (0.4–1.0 ppm) used to maintain the effluent values in the range of 0.2–0.3 ppm in the large autoclave system.

Table 13. Crack Growth Results for a Sensitized Type 304 SS Specimen[a] during Experiments[b] at 289°C in Water Containing 0.2–0.3 ppm Dissolved Oxygen[c], Carboxylic Acids, and Impurity Anions

		Water Chemistry						Electrode Potential		Type 304 SS	
Test No.	Test Time, h	Organic Acid	Conc., ppm	Impurity Anion[e]	Conc., ppb	pH at 25°C	Cond., $\mu S \cdot cm^{-1}$	304 SS, mV(SHE)	Pt, mV(SHE)	K_{max}[d] $MPa \cdot m^{1/2}$	Growth Rate, $m \cdot s^{-1}$
1	141 1458	–	–	–	–	6.50	0.13	195	200	30.4	2.9×10^{-10}
2	1458 2465	Propionic	0.1	–	–	5.95	0.48	190	190	31.4	2.9×10^{-10}
3	2465 3452	Propionic	1.0	–	–	5.17	3.0	206	220	31.6	0.2×10^{-10}
4	3452 4680	–	–	–	–	6.53	0.12	190	200	33.6	2.9×10^{-10}
5	4680 5836	Butyric	1.0	–	–	5.27	2.5	170	180	33.6	~0
6	5836 7182	Butyric	0.1	–	–	6.18	0.38	180	190	34.8	1.9×10^{-10}
7	7182 7566	Butyric	1.0	Sulfate	100	5.18	3.7	190	190	37.0	7.4×10^{-10}
8	7566 8188	Butyric	1.0	–	–	5.23	3.0	190	230	37.0	~0
9	8188 9341	Butyric	1.0	Chloride	100	5.21	3.2	200	210	39.8	1.5×10^{-10}
10	9341 10490	Butyric	1.0	–	–	5.16	3.1	175	220	39.8	~0

[a] Compact tension specimen (1TCT). AISI 304 SS (Heat No. 30956; Specimen No. 30) received the following heat treatment: solution-anneal at 1050°C for 0.5 h plus 700°C for 0.25 h plus 500°C for 24 h (EPR = 2 $C \cdot cm^{-2}$).

[b] Frequency and load ratio, R, for the positive sawtooth waveform were 8×10^{-2} Hz and 0.95, respectively.

[c] Effluent dissolved-oxygen concentration; feedwater oxygen concentration was 0.4–1.0 ppm.

[d] Stress intensity, K_{max}, values at the end of the test condition.

[e] Sulfate and chloride added as H_2SO_4 and NaCl.

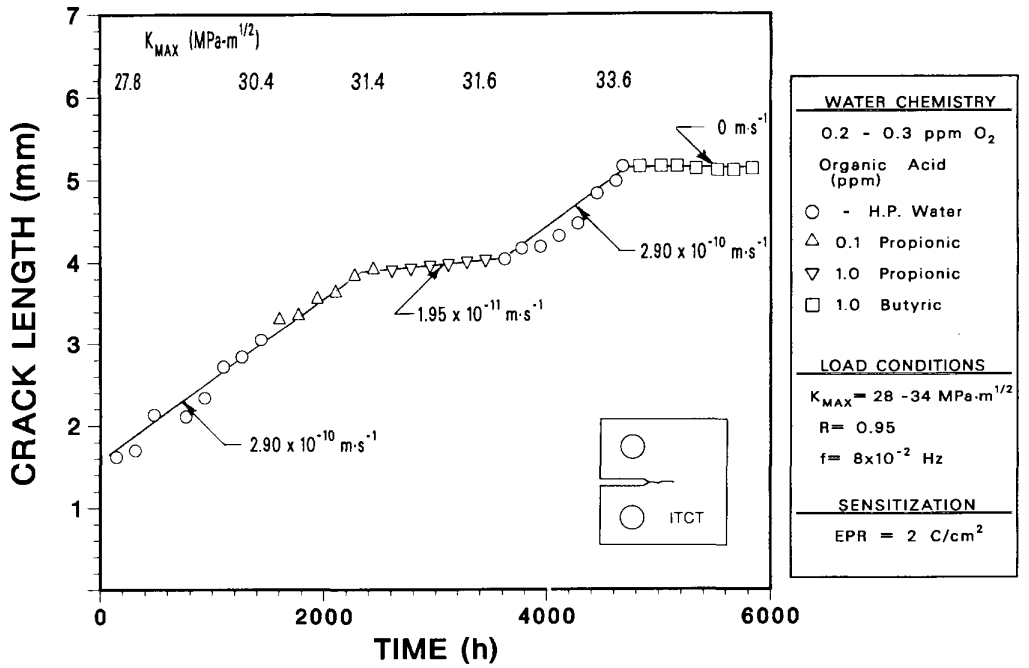

Figure 15. Crack Length versus Time for a 1TCT Specimen of Sensitized (EPR = 2 C/cm^2) Type 304 SS in Oxygenated Water (0.2–0.3 ppm) without and with 0.1 and 1.0 ppm Propionic Acid at 289°C.

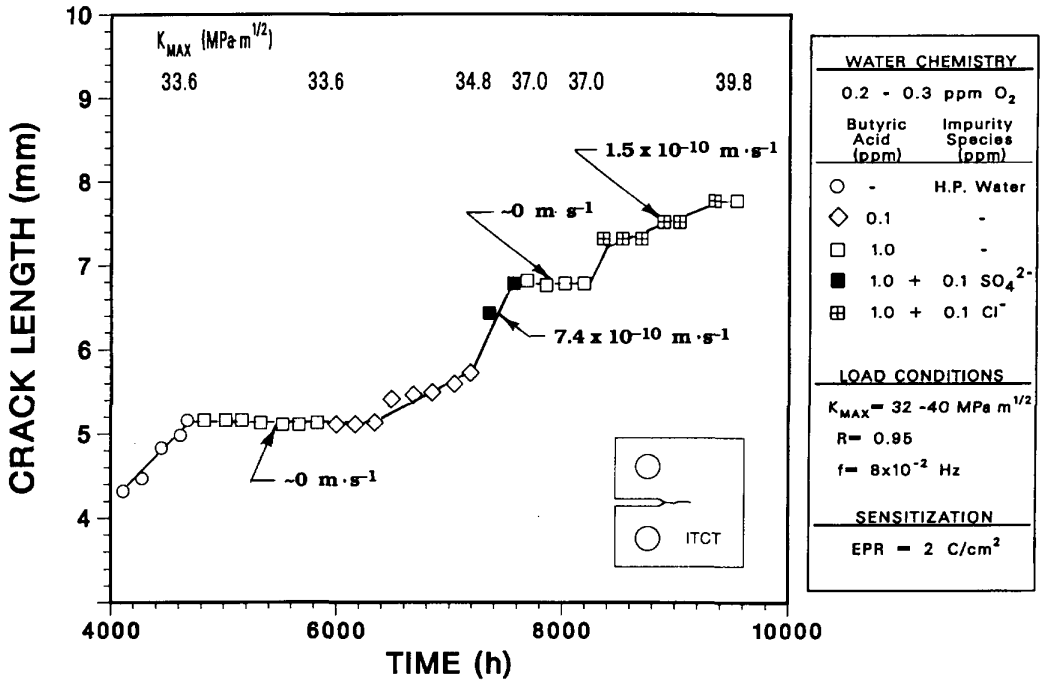

Figure 16. Crack Length versus Time for a Continuation of the Test on a 1TCT Specimen of Sensitized (EPR = 2 C/cm^2) Type 304 SS in Oxygenated Water (0.2–0.3 ppm) without and with 0.1 ppm Butyric Acid, and 1.0 ppm Butyric Acid without and with 100 ppb of Sulfate or Chloride at 289°C.

A mechanism has been determined whereby the organic acids could inhibit SCC in oxygenated water even though the ECP regime of the steel is conducive to cracking (>–250 mV[SHE] at 289°C). It is known that many organic substances such as aliphatic alcohols and acids, carboxylic acids, and others adsorb on metal and oxide electrodes at very high potentials associated with oxygen evolution at ambient temperature.[34–38] The rate constant for oxygen evolution is independent of the presence of the inhibitor, i.e., the effect of the inhibitor was mainly to block active reaction sites.[34] The adsorbability of the various substances increases as the molecular weight increases,[35,36] and the adsorption follows a logarithmic isotherm at concentrations $\geq 10^{-5}$ M (≥ 1 ppm).[36–38] It is plausible that carboxylic acids, at a similar concentration in the water, adsorb on the oxide surface of Type 304 SS and inhibit oxygen reduction, which is the cathodic partial process that couples with anodic dissolution at the crack tip in a slip–dissolution mechanism[23,24] of crack growth.

The pronounced effect of these substances on crack growth can be rationalized from the mechanism of oxygen reduction on electrode surfaces. Cathodic reduction of oxygen is a complex electrochemical process that can proceed along two reaction paths according to the nature of the electrode material, the electrolyte, and the reaction conditions, i.e., a direct $4e^-$ path described by the equation

$$O_2 + 2H_2O + 4e^- = 4OH^- \qquad (10)$$

or by two consecutive $2e^-$ steps that are represented by the equations

$$O_2 + H_2O + 2e^- = HO_2^- + OH^- \qquad (11)$$

$$HO_2^- + H_2O + 2e^- = 3OH^-. \qquad (12)$$

Both the direct $4e^-$ and sequential $2e^-$ paths have been reported for various electrode–electrolyte systems.[39–45] If oxygen reduction occurs through a $4e^-$ path, adsorption occurs through a bridged configuration in which each adsorbed molecule requires two adjacent vacant sites[44,45] as depicted by the equation

$$2M + O_2 = M\begin{array}{c}O-O\\ \diagup \quad \diagdown\end{array}M \quad (O_2 \text{ adsorbed}). \qquad (13)$$

From reaction rate theory, the rate of reduction is first-order in the concentration of dissolved oxygen, C_{O_2}, but second-order in fractional coverage of empty sites; i.e.,

$$\Theta_o = K_{eq}\,[C_{O_2}]\,[\Theta_m]^2,\ C_{O_2} \qquad (14)$$

where Θ_o and Θ_m are fractional surface coverage of O_2 and empty sites, respectively. For a $2e^-$ path, oxygen adsorption occurs via an end-on configuration[44,45] depicted by the equation

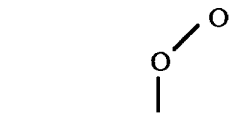

$$M + O_2 = M \qquad (O_2 \text{ adsorbed}) \tag{15}$$

where the rate of reduction is first-order with respect to O_2 concentration and the vacant sites, i.e.,

$$\Theta_o = K_{eq} [C_{O_2}] \Theta_m. \tag{16}$$

Equations (14) and (16) suggest that a decrease in available sites, Θ_m, by adsorption of organic species would have a more significant effect on the available sites for oxygen reduction, Θ_o, for a $4e^-$ reduction path than on a $2e^-$ path for the same dissolved-oxygen concentration.

Previous results[19,20] indicated that the CGR of the steel follows a 1/4-power dependence over several orders of magnitude of the oxygen concentration, i.e., a $4e^-$ process according to Eq. (10), in contrast to a $2e^-$ path (Eqs. [11] or [12]) where a 1/2-power dependence would have been observed, as is observed in the case of the reduction of sulfate to sulfite, which is a $2e^-$ process.

With the cathodic reduction of oxygen as the rate-controlling process for SCC at a fixed strain rate, and the relationship between the fractional surface coverage of oxygen available for this reaction (Eq. [14]), one can rationalize the strong mitigating effect of the various organic species on the CGR of the steel in oxygenated water. For example, a decrease in the value of Θ_m from 1.0 (high-purity water) to ~0.3 or 0.1 by blockage of ~70 or 90% of the available sites would decrease Θ_o by a factors of ~10 or 100, respectively. For comparison, the CGRs of the steel in the CERT experiments in Table 12 decreased by factors of ~4 to 5 relative to high-purity water, which suggests that <70% of the sites were blocked by the higher molecular weight carboxylic acids at a concentration of 1.0 ppm. However, at this concentration the results of the fracture-mechanics tests in Table 13 and Figs. 15 and 16 indicate at least an order-of-magnitude decrease in the CGRs (i.e., $< 2 \times 10^{-11}$ m·s^{-1}) relative to high-purity water.

The inability of the organic species (i.e., butyric acid) to mitigate SCC when sulfate is present in the water is consistent with the site blockage mechanism, since site blockage is not as effective for $2e^-$ reduction process, e.g., Eq. (16). Because the chloride ion does not undergo cathodic reduction, its deleterious effect on SCC in oxygenated water containing the organic acid must be attributed to other mechanisms. These include: (1) adsorption of chloride ions may decrease surface coverage by the inhibitor,[46,47] (2) chloride could act as an "anion bridge" for electron transfer across the oxide/electrolyte interface that accelerates redox reactions,[48-51] and (3) chloride may be incorporated into the oxide film and alter the passivity and transport properties.[52,53]

4 Environmentally Assisted Cracking of Ferritic Steels

Plain carbon steels are used extensively in PWR and BWR nuclear steam supply systems as piping and pressure vessel materials. The steels of interest for these applications include A106–Gr B and A333–Gr 6 for seamless pipe and A302–Gr B, A508–2, and A533–Gr B plate for pressure vessels. Although operating experience with ferritic steel components in reactor pressure boundaries is considerably better than with weld–sensitized austenitic stainless steels, instances of cracking of ferritic steels have occurred in plants in the U.S. and abroad.

Ferritic steels become susceptible to TGSCC in high–temperature water containing dissolved oxygen, and some evidence suggests a synergistic effect between oxygen and soluble copper compounds (e.g., $CuCl_2$) as well as other impurities to produce susceptibility to SCC. However, the ranges of dissolved oxygen and impurity concentrations that can lead to SCC in these materials remain relatively ill–defined. The objective of this work is to characterize the environmental and material conditions that can produce SCC susceptibility in these steels.

4.1 Technical Progress

4.1.1 Constant–Extension–Rate Tensile Tests (J. Y. Park)

The results of CERT tests on several types of ferritic steel (A333, A106, A155, A516, and A533B) are summarized in Table 14. The tests were performed in deoxygenated water (~5–25 ppb) at 289°C with 100 ppb sulfate (as H_2SO_4) at strain rates of 1.0×10^{-6}, 5.0×10^{-7}, and 2.5×10^{-7} s^{-1}. All materials showed TGSCC on the fracture surfaces, except for A533B. However, A533B also showed TGSCC when the strain rate was decreased to 2.5×10^{-7} s^{-1}. The average crack growth rates varied from 1×10^{-9} to 9×10^{-9} $m \cdot s^{-1}$. The results of the current tests can be compared with previous CERT results[54] in water with 0.2–0.5 ppm oxygen. Although there is substantial scatter in the data, overall the crack growth rates are lower in the low–oxygen environment, and the A533B steel appears to be less susceptible to cracking.

As expected from related work on the fatigue crack growth of ferritic steels in reactor environments,[55,56] there appears to be a strong correlation between the sulfur content of the steel (particularly the presence of sulfide inclusions) and susceptibility to SCC. There are far fewer inclusions in the less susceptible A533B steel than in the more susceptible materials. Fractographic evidence in Fig. 17 also indicates that SCC initiates at inclusion sites in a A516–Gr 7 steel specimen (Heat No. DP2–F34) after a test in water with <25 ppb oxygen and 100 ppb sulfate.

4.1.2 Crack–Growth–Rate Tests (J. Y. Park, W. E. Ruther, and T. F. Kassner)

Fracture–mechanics CGR tests are being performed on specimens from a plate of A533–Gr B pressure vessel steel (Heat No. 02, containing 0.018% sulfur and 0.012% phosphorus) in deionized water with 0.2 –0.3 ppm dissolved oxygen at 289°C. One test involves a composite 1TCT specimen of the ferritic steel/Inconel–182/Inconel–600, which was fabricated by overlaying the ferritic steel with In–182 weld metal and then electron–beam welding In–600 to the In–182. The specimen is designed so that the crack will proceed

Table 14. CERT Data on Ferritic Steels in Water with 100 ppb Sulfate and <25 ppb Oxygen at 289°C

Material Heat No.	Specimen No.	Strain Rate, s^{-1}	Max Load, MPa	T_f, h	RA, %	Elong., %	Crack Growth, $m \cdot s^{-1}$	ECP, mV(SHE)
A106-Gr B DP2-F29	29B-8	1.0×10^{-6}	557	54.8	32.7	19.3	5.9×10^{-9}	-147
"	29B-9	"	554	66.1	35.4	24.7	5.0×10^{-9}	-136
A106-Gr B DP2-F30	30C-9	2.5×10^{-7}	604	200.1	22.2	18.7	4.8×10^{-9}	-131
A155-CK70 DP20F26	26-5	5.0×10^{-7}	525	131.2	31.6	22.8	2.0×10^{-9}	-144
"	26-6	2.5×10^{-7}	527	280.5	63.7	26.0	1.1×10^{-9}	-47
"	26-8	"	523	249.0	32.6	22.6	1.3×10^{-9}	+19
SA333-Gr6	F9-6	5.0×10^{-7}	539	134.1	37.7	23.3	3.1×10^{-9}	-137
A533-Gr B A5401	W7-6	1.0×10^{-6}	653	61.2	73.7	21.9	Ductile	-146
"	W7-8	"	650	61.6	73.1	22.6	Ductile	-197
"	W7-10	5.0×10^{-7}	654	124.5	73.1	23.3	Ductile	-126
"	W7-11	2.5×10^{-7}	658	168.9	46.9	13.5	3.1×10^{-9}	-153
"	W7-12	"	659	207.7	46.3	18.1	2.3×10^{-9}	-172
A533-Gr B XE5-M	5M-8	1.0×10^{-6}	605	70.1	71.4	25.4	Ductile	-140
"	5M-10	"	602	64.8	69.2	24.3	Ductile	-157
"	5M-11	5.0×10^{-7}	609	122.0	68.0	21.6	Ductile	-192
"	5M-13	2.5×10^{-7}	606	241.4	52.7	21.5	1.9×10^{-9}	-141
"	5M-14	"	608	227.5	53.2	20.1	2.1×10^{-9}	-47
A516-Gr70 DP2-F34	34-6A	1.0×10^{-6}	500	85.2	35.4	31.3	5.8×10^{-9}	-157
"	34-7B	"	499	69.1	47.2	27.2	8.9×10^{-9}	-130

from the In-182 into the ferritic steel. The specimen was nickel plated to prevent contact of the large surface of low-alloy steel with the environment in order to simulate a crack in a clad low-alloy steel vessel.

In another test system, a conventional 1TCT ferritic specimen, a nickel-plated specimen and a gold-plated specimen are being tested. The plated specimens are included in order to determine whether electron transfer through the oxide film on the bulk surface of the ferritic steel is important in the overall SCC process, and hence, to assess the validity of using data obtained from specimens without cladding to analyze the behavior of a clad ferritic vessel, where only the crack surface is exposed to the environment. The composite specimen is intended to address whether the K_{ISCC} value determined from conventional fatigue precracked specimens is applicable to the more prototypical case when a crack in the ferritic steel initiates from a stress corrosion crack in the In-182 weld metal.

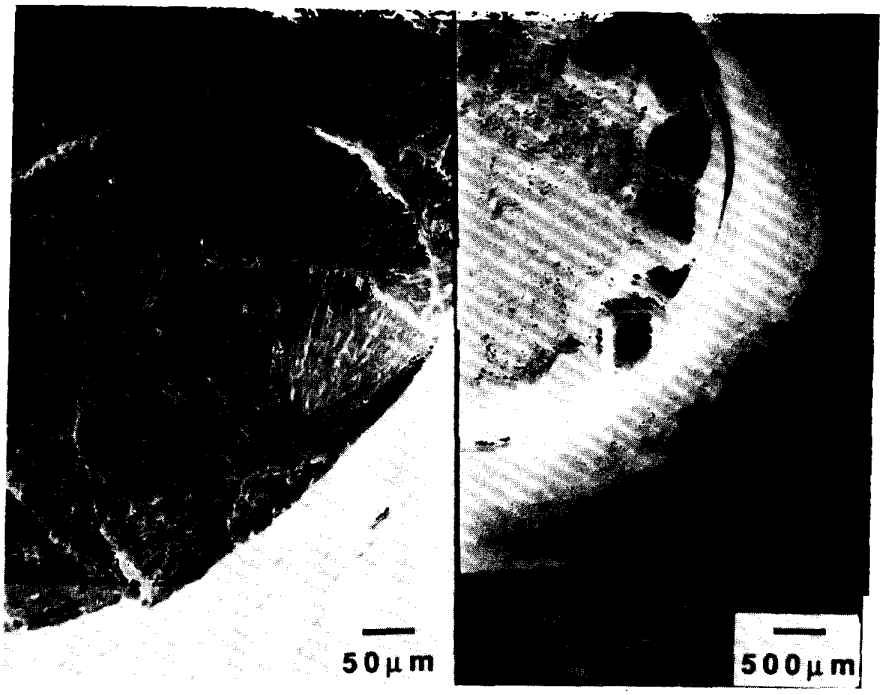

Figure 17. Fracture Surface of A516-Gr 7 Ferritic Steel CERT Specimen (Heat No. DP-2F34 Specimen No. 34-6A) after a Test in Water with 100 ppb Sulfate and <25 ppb Oxygen at 289°C. Initiation of transgranular cracking at inclusion sites is evident.

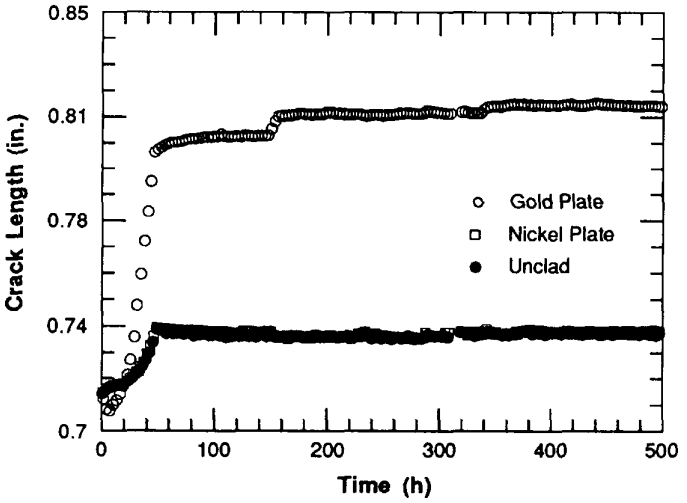

Figure 18.
Crack Length versus Time for Au- and Ni-Plated and Non-Plated (Bare) 1TCT Specimens of A533-Gr B Carbon Steel in Deionized, Oxygenated Water at 289°C.

The composite specimen fatigue was precracked in the environment and the SCC test was initiated at a load ratio of 0.95, a frequency of 0.08 Hz, and a K_{max} of 28 MPa·m$^{1/2}$. Crack growth in the In-182 weld metal of the composite specimen occurred at a rate of 2.5 x 10^{-10} m·s^{-1} for the first 1800 h, i.e., a rate typical of austenitic SS under similar loading conditions. Crack length measurements indicate that the crack tip reached the

interface between the In-182 weld metal and the low-alloy steel, but did not enter the ferritic material. The K_{max} value was then increased to 35 MPa·m$^{1/2}$ to determine if cracking would resume at the higher stress intensity. Because no sustained crack growth was observed at this stress intensity level, the K_{max} value was then increased to 40 MPa·m$^{1/2}$, and again no sustained crack growth was observed. The tests are still ongoing and the stress intensity levels will be increased until sustained crack growth is observed.

In the other system, the conventional and the nickel- and gold-plated specimens were precracked under a cyclic load (a sawtooth wave shape with 12-s loading and 1-s unloading time) of R = 0.25 at 0.08 Hz and a maximum initial stress intensity of 20 MPa·m$^{1/2}$. During this precracking phase the crack growth rates were 4 x 10^{-9} m·s^{-1} for the bare and nickel-plated specimens and 2 x 10^{-8} m·s^{-1} for the gold-plated specimen, i.e., the gold-plated specimen had a crack growth rate a factor of 5 larger than the other specimens. The crack length, determined by the DC potential method, is plotted versus test time in Fig. 18. After fatigue precracking, the load ratio was changed to R = 0.95 and the crack growth tests were continued in the same environment. No crack growth was observed in any of the specimens for stress intensity values up to 30 MPa·m$^{1/2}$.

5 Summary of Results

Major findings from work on environmentally assisted cracking of LWR materials during this reporting period are summarized below.

5.1 Influence of Sulfate on SCC of Types 316NG and 304 SS

- A SCC model developed by Ford et al.[11] tends to overpredict the effect of conductivity on the CGR of sensitized Type 304 SS on the basis of our experimental data; however, overall predictions from the model are reasonably good.

5.2 Fatigue of Type 316NG SS In Simulated BWR Water

- The normalized fatigue life N_{env}/N_{air} of Type 316NG SS depends primarily on the strain rate and is relatively independent of strain range.

- At the lowest strain rates, the fatigue life in the environment is about one-third of that in air, but the data are too limited to assess whether the strain-rate effect has reached saturation.

- A comparison of the results on Type 316NG SS with similar data obtained by Iida et al.[15] for an A333-Gr 6 steel indicates that the A333 steel shows a stronger strain-rate dependence and a more severe reduction in fatigue life in oxygenated water.

5.3 Water Chemistry Influence on SCC of Sensitized Type 304 SS

- Chromate acts in a similar manner to other oxyanions in its effect on SCC of sensitized Type 304 SS. This species undergoes cathodic reduction and contributes to crack growth by scavenging electrons produced by anodic dissolution of metal at the crack tip in a slip-dissolution mechanism[23,24] of crack advance.

- In comparison with other species at the 100 ppb level in simulated BWR water, chromate is less deleterious than sulfur species and more deleterious than nitrate, borate, carbonate, and chloride in CERTs at 289°C and a strain rate of 1×10^{-6} s^{-1}.

- Results of this and other investigations[57,58] indicate that carbonic and carboxylic (acetic, formic, lactic, oxalic, propionic, and butyric) acids at low concentrations (~1 ppm) do not have a deleterious effect on IGSCC of sensitized Type 304 SS under simulated normal BWR water chemistry.

- Short-chain carboxylic acids mitigate IGSCC of the steel under high-R, low-frequency loading at stress intensity values of <40 MPa·$m^{1/2}$.

- The role of the organic acids at low concentrations in oxygenated water in mitigating SCC of sensitized Type 304 SS primarily involves adsorption on and blockage of active sites for the cathodic reduction of oxygen, in contrast to that of commonly used chemical organic oxygen scavengers, which decrease both the dissolved oxygen concentration and the ECP of steel (and platinum) to very low values.

- Site blockage by carboxylic acids (butyric) was not effective in mitigating IGSCC when other ionic species (sulfate or chloride) were present in the oxygenated water at low concentrations (~100 ppb).

- Surface reactions involving organic substances, dissolved oxygen, and various ionic species in high-temperature water contribute to the complex nature of IGSCC of sensitized Type 304 SS, and under certain conditions can predominate over concomitant mechanical and electrochemical processes at the crack tip.

5.4 SCC of Ferritic Steels

- A comparison of current results in deoxygenated water (~5–25 ppb) with CERT previous results[54] in the water with 0.2–0.5 ppm oxygen, with and without sulfate addition to the feedwater, indicates that overall the crack growth rates are lower in the low-oxygen environment, and the A533B steel appears to be less susceptible to cracking than other ferritic steels.

- As expected from related work on the fatigue crack growth of ferritic steels in reactor environments,[55,56] there appears to be a strong correlation between the sulfur content of the steel (particularly the presence of sulfide inclusions) and susceptibility to SCC. Inclusions are far fewer in the less susceptible A533B steel than in the more susceptible materials.

- Fracture-mechanics crack growth rate tests are being performed on A533-Gr B steel and on a composite specimen that was fabricated by overlaying the ferritic steel with In-182 weld metal to address the question of whether the K_{ISCC} value determined from conventional fatigue precracked specimens is applicable to the more prototypical case when a crack in the ferritic steel initiates from a stress

corrosion crack in the In-182 weld metal. No sustained crack growth has been observed in the ferritic steel at a stress intensity level of 40 MPa·m$^{1/2}$.

References

1. W. E. Ruther, W. K. Soppet, and T. F. Kassner, in *Environmentally Assisted Cracking in Light Water Reactors: Semiannual Report, April - September 1985*, NUREG/CR-4667 Vol. 1, ANL-86-31, pp. 27-52 (June 1986).

2. W. E. Ruther, W. K. Soppet, and T. F. Kassner, in *Materials Science and Technology Division Light-Water-Reactor Safety Research Program: Quarterly Progress Report, October - December 1983*, NUREG/CR-3689 Vol. IV, ANL-83-85 Vol. IV, pp. 75-87 (August 1984).

3. W. E. Ruther, W. K. Soppet, and T. F. Kassner, in *Environmentally Assisted Cracking in Light Water Reactors: Annual Report, October 1983 - September 1984*, NUREG/CR-4287, ANL-85-33, pp. 110-113 (June 1985).

4. W. E. Ruther, W. K. Soppet, J. Y. Park, and T. F. Kassner, in *Environmentally Assisted Cracking in Light Water Reactors: Semiannual Report, April - September 1986*, NUREG/CR-4667 Vol. III, ANL-87-37, pp. 2-7 (September 1987).

5. W. E. Ruther, W. K. Soppet, J. Y. Park, and T. F. Kassner, in *Environmentally Assisted Cracking in Light Water Reactors: Semiannual Report, October 1986 - March 1987*, NUREG/CR-4667 Vol. IV, ANL-87-41, pp. 2-10 (December 1987).

6. W. E. Ruther, W. K. Soppet, J. Y. Park, and T. F. Kassner, in *Environmentally Assisted Cracking in Light Water Reactors: Semiannual Report, April - September 1987*, NUREG/CR-4667 Vol. V, ANL-88-32, pp. 3-9 (February 1989).

7. W. E. Ruther, W. K. Soppet, J. Y. Park, and T. F. Kassner, in *Environmentally Assisted Cracking in Light Water Reactors: Semiannual Report, October 1987 - March 1988*, NUREG/CR-4667 Vol. VI, ANL-89/10, pp. 5-14 (August 1989).

8. J. Y. Park and W. J. Shack, in *Light-Water-Reactor Safety Research Programs: Quarterly Progress Report, October - December 1984*, NUREG/CR-3998 Vol. III, ANL-84-60 Vol. III, pp. 7-14 (October 1985).

9. J. Y. Park and W. J. Shack, in *Light-Water-Reactor Safety Research Programs: Quarterly Progress Report, January - March 1985*, NUREG/CR-4490 Vol. I, ANL-85-75 Vol. I, pp. 14-16 and 43-49 (March 1986).

10. W. E. Ruther, W. K. Soppet, J. Y. Park, and T. F. Kassner, in *Materials Science and Technology Division Light-Water-Reactor Safety Research Program: Quarterly Progress Report, April - June 1983*, NUREG/CR-3689 Vol. II, ANL-83-85 Vol. II, pp. 44-48 (June 1984).

11. F. P. Ford, D. F. Taylor, P. L. Andresen, and R. Ballinger, "Corrosion-Assisted Cracking of Stainless and Low-Alloy Steels," EPRI NP-5064S (February 1987)

12. V. N. Shah and P. E. MacDonald, "Residual Life Assessment of Major Light Water Reactor Components–Overview Volume 1," NUREG/CR–4731 EGG–2469 Vol. 1 (June 1987).

13. H. S. Mehta, S. Ranganath, and D. Weinstein, "Application of Environmental Fatigue Stress Rules to Carbon Steel Reactor Piping," EPRI NP–4644M Vols. 1 and 2 (July 1986).

14. D. A. Hale, S. A. Wilson, E. Kiss, and A. J. Gianuzzi, "Low–Cycle Fatigue Evaluation of Primary Piping Materials in a BWR Environment," GEAP–20244 (September 1977).

15. K. Iida, H. Kobayashi, and M. Higuchi, "Predictive Method of Low Cycle Fatigue Life of Carbon and Low Alloy Steels in High Temperature Water Environments," in Proc. of the 2nd Int. Atomic Energy Agency Specialists' Meeting on Subcritical Crack Growth, NUREG/CP–0067, Vol 2, April 1986.

16. G. E. Brobst, "Chromate Substitutes for Corrosion Inhibitors in Cooling Systems," EPRI NP–5569 (December 1987).

17. W. E. Ruther, W. K. Soppet, and T. F. Kassner, in *Environmentally Assisted Cracking in Light Water Reactors: Semiannual Report, April – September 1987*, NUREG/CR–4667 Vol. V, ANL–88–32 (February 1989), pp. 24–37.

18. W. E. Ruther, W. K. Soppet, and T. F. Kassner, in *Environmentally Assisted Cracking in Light Water Reactors: Semiannual Report, October 1987 – March 1988*, NUREG/CR–4667 Vol. 6, ANL–89/10 (August 1989), pp. 27–42.

19. W. E. Ruther, W. K. Soppet, and T. F. Kassner, in *Light–Water–Reactor Safety Research Programs: Quarterly Progress Report, January – March 1985*, NUREG/CR–4490 Vol.I, ANL–85–75 Vol. I (March 1986), pp. 25–42.

20. W. E. Ruther, W. K. Soppet, and T. F. Kassner, in *Environmentally Assisted Cracking in Light Water Reactors: Semiannual Report, April – September 1985*, NUREG/CR–4667 Vol. I, ANL–86–31 (June 1986), pp. 27–41.

21. H. D. Solomon, *Corrosion* **40**, 493–506 (1984).

22. W. E. Ruther, W. K. Soppet, and T. F. Kassner, *Corrosion* **44**, 791–799 (1988).

23. F. P. Ford, "Stress Corrosion Cracking," in *Corrosion Processes*, R. N. Parkins, ed., Applied Science Publishers, New York, (1982), pp. 271–309.

24. D. A. Vermilyea, in *Proc. Intl. Conf. on Stress Corrosion Cracking and Hydrogen Embrittlement of Iron Base Alloys*, R. W. Staehle, J. Hochmann, R. D. McCright, and J. E. Slater, eds., NACE, Houston (1983), p. 208.

25. B. H. Dillman, R. A. Reed, and C. C. Lin, "BWR Coolant Impurity Identification Study, Final Report," EPRI NP–4156 (August 1985).

26. B. H. Dillman, J. C. Elliot, R. A. Head, J. E. Osterle, and R. S. Tunder, "Monitoring of Chemical Contaminants in BWRs," Final Report, EPRI NP-4134 (July 1985).

27. J. E. Richards and W. A. Byers, "Industry-wide Survey of PWR Organics, Final Report," EPRI NP-4698 (July 1986).

28. S. D. Strauss, "Advances in Chemical Water Treatment Improve Reliability of Steam-Generating Systems," *Power*, (October 1986), pp. 15-20.

29. "PWR Secondary Water Chemistry Guidelines, Revision 1," EPRI NP-5056-SR, Electric Power Research Institute, Palo Alto, CA (March 1987).

30. "BWR Hydrogen Water Chemistry Guidelines: 1987 Revision," EPRI NP-4947-SR, Electric Power Research Institute, Palo Alto, CA (October 1988).

31. J. N. Kass and R. L. Cowan, "Hydrogen Water Chemistry for BWRs," in *Environmental Degradation of Materials in Nuclear Power Systems-Water Reactors, Proc. of the 2nd Int. Symp.*, Monterey, CA, September 9-12, 1985, ANS, La Grange Park, IL (1986), pp. 211-218.

32. M. E. Indig, B. M. Gordon, R. B. Davis, and J. E. Weber, "Evaluation of In-reactor Stress Corrosion Cracking via Electrochemical Measurements," ibid., pp. 411-418.

33. D. D. Macdonald and G. Cragnolino, "The Critical Potential for IGSCC of Sensitized Type 304 SS in High Temperature Aqueous Systems," ibid., pp. 426-434.

34. Yu. M. Tyurin, G. F. Volodin, and V. S. Paducheva, *Elektrokhimiya* **7**, 1309-1312 (1971).

35. V. I. Naumov, L. A. Smirnova, G. N. Afon'shin, and Yu. M. Tyurin, *Elektrokhimiya* **7**, 1872-1876 (1971).

36. Yu. M. Tyurin, V. I. Naumov, Vyach. N. Flerov, and Yu. V. Battalova, *Elektrokhimiya* **10**, 1119-1123 (1974).

37. V. I. Naumov and Yu. M. Tyurin, *Elektrokhimiya* **8**, 1220-1223 (1972).

38. Yu. M. Tyurin, G. F. Volodin, L. A. Smirnova, and Yu. V. Battalova, *Elektrokhimiya* **9**, 532-536 (1973).

39. P. K. Adanuvor and R. E. White, *J. Electrochem. Soc.* **134**, 1093-1098 (1987).

40. P. K. Adanuvor and R. E. White, *J. Electrochem. Soc.* **135**, 2509-2516 (1988).

41. V. Jovancicevic and J. O'M. Bockris, *J. Electrochem. Soc.* **133**, 1797-1807 (1986).

42. L. M. Vracar and D. B. Sepa, *J. Electrochem. Soc.* **133**, 1835-1839 (1986).

43. E. J. Taylor, N. R. K. Vilambi, and A. Gelb, *J. Electrochem. Soc.* **136**, 1939-1944 (1989).

44. J. C. Huang, R. K. Sen, and E. Yeager, *J. Electrochem. Soc.* **126**, 786–792 (1979).

45. S. M. Kaska, S. Sarangapani, and Jose Giner, *J. Electrochem. Soc.* **136**, 79–83 (1989).

46. T. Murakawa and N. Hackerman, *Corros. Sci.* **4**, 387–396 (1964).

47. K. Aramaki, T. Mochizuki, and H. Nishihara, *J. Electrochem. Soc.* **135**, 2427–2432 (1988).

48. J. P. Cushing and A.T. Hubbard, *J. Electroanal. Chem.* **23**, 183–203 (1969).

49. R. de Levie and L. Pospisil, *J. Electroanal. Chem.* **25**, 340–341 (1970).

50. R. R. Dogonadze, J. Ulstrup, and Yu. I. Kharkats, *J. Electroanal. Chem.* **39**, 47–61 (1972).

51. N. C. Hung and Z. Nagy, *J. Electrochem. Soc.* **134**, 2215–2220 (1987).

52. T. Okada, *J. Electrochem. Soc.* **131**, 241–247 (1984).

53. J. R. Galvele, "Present State of Understanding of the Breakdown of Passivity and Repassivation," in *Passivity of Metals*, R. P. Frankenthal and J. Kruger, eds., The Electrochemical Soc., Inc., Princeton, NJ, (1978), pp. 285–327.

54. J. Y. Park, in *Environmentally Assisted Cracking in Light Water Reactors: Semiannual Report, October 1987–March 1988*, NUREG/CR–4667 Vol. 6, ANL–89–10, pp. 43–47 (August 1989).

55. J. H. Bulloch, "The Effect of Sulfide Distribution and Morphology on Environmentally Assisted Cracking Behavior of Ferritic Reactor Pressure Vessel Materials," in *Proc. of the 3rd Int. Symp. on Environmental Degradation of Materials in Nuclear Power Systems–Water Reactors*, G. J. Theus and J. R. Weeks, eds., American Nuclear Society, LaGrange Park, IL, 1988.

56. P. M. Scott, A. E. Truswell, and S. G. Bruce, *Corrosion* **40**, 350–357 (1984).

57. T. Christman and G. Cragnolino, *Corrosion* **44**, 345–353 (1988).

58. L. Ljungberg, D. Cubicciotti, and M. Trolle, *Corrosion* **45**, 215–222 (1989).

NRC FORM 335 (2-89) NRCM 1102, 3201, 3202

U.S. NUCLEAR REGULATORY COMMISSION

BIBLIOGRAPHIC DATA SHEET

(See instructions on the reverse)

1. REPORT NUMBER (Assigned by NRC, Add Vol., Supp., Rev., and Addendum Numbers, if any.)
NUREG/CR-4667 Vol. 7
ANL-89/40

2. TITLE AND SUBTITLE
Environmentally Assisted Cracking in Light Water Reactors

Semiannual Report
April 1988-September 1988

3. DATE REPORT PUBLISHED
MONTH: March
YEAR: 1990

4. FIN OR GRANT NUMBER
A2212

5. AUTHOR(S)
W. J. Shack, T. F. Kassner, J. Y. Park,
W. E. Ruther, W. K. Soppet

6. TYPE OF REPORT
Technical; Semiannual

7. PERIOD COVERED *(Inclusive Dates)*
April-September 1988

8. PERFORMING ORGANIZATION – NAME AND ADDRESS *(If NRC, provide Division, Office or Region, U.S. Nuclear Regulatory Commission, and mailing address; if contractor, provide name and mailing address.)*

Argonne National Laboratory
9700 South Cass Avenue
Argonne, IL 60439

9. SPONSORING ORGANIZATION – NAME AND ADDRESS *(If NRC, type "Same as above"; if contractor, provide NRC Division, Office or Region, U.S. Nuclear Regulatory Commission, and mailing address.)*

Division of Engineering
Office of Nuclear Regulatory Research
U. S. Nuclear Regulatory Commission
Washington, D. C. 20555

10. SUPPLEMENTARY NOTES

11. ABSTRACT *(200 words or less)*

This report summarizes work performed by Argonne National Laboratory on environmentally assisted cracking in light water reactors during the six months from April to September 1988. The stress corrosion cracking (SCC) of Types 316NG and 304 stainless steels (SSs) was investigated by means of slow-strain-rate and fracture-mechanics crack-growth-rate tests in high-temperature water. The effects of load ratio and water chemistry on the crack growth behavior of Type 316NG and sensitized Type 304 SS were determined in long-term fracture-mechanics tests. The influence of organic impurities on the SCC of sensitized Type 304 SS was also investigated. Fatigue tests were conducted on Type 316NG SS in air and simulated boiling water reactor water at 288°C to assess the degree of conservatism in the ASME Code Section III fatigue design curves. An ongoing investigation of the susceptibility of several heats of different grades of low-alloy ferritic steels to transgranular SCC in slow-strain-rate and fracture-mechanics tests was continued.

12. KEY WORDS/DESCRIPTORS *(List words or phrases that will assist researchers in locating the report.)*
Water Chemistry
Corrosion
Stress Corrosion Cracking
Crack Growth

13. AVAILABILITY STATEMENT
Unlimited

14. SECURITY CLASSIFICATION
(This Page)
Unclassified
(This Report)
Unclassified

15. NUMBER OF PAGES
56

16. PRICE

Distribution for NUREG/CR-4667 Vol. 7 (ANL-89/40)

Internal:

W. J. Shack (30)

TIS File (3)

ANL Libraries (2)

ANL Patent File

ANL Contract File

External:

NRC, for distribution per R5 (315)

Manager, Chicago Operations Office, DOE

Materials and Components Technology Division Review Committee:

- P. A. Alexander, Lord Corp., Erie, PA
- M. S. Dresselhaus, Massachusetts Institute of Technology, Cambridge, MA
- S. J. Green, Electric Power Research Institute, Palo Alto, CA
- R. A. Greenkorn, Purdue University, West Lafayette, IN
- L. J. Jardine, Lawrence Livermore National Laboratory, CA
- C.-Y. Li, Cornell University, Ithaca, NY
- R. E. Scholl, Counter Quake Corp., Redwood City, CA
- P. G. Shewmon, Ohio State University, Columbus, OH
- Richard Smith, EPRI NDE Center, Charlotte, NC

P. L. Andresen, General Electric Corporate Research and Development, Schenectady, NY

W. H. Bamford, Structural Materials Engineering, Westinghouse Electric Corp., Pittsburgh, PA

R. M. Crawford, Fluor-Daniel Corp., Chicago, IL

D. Cubicciotti, Electric Power Research Inst., Palo Alto, CA

W. H. Cullen, Materials Engineering Assoc., Inc., Lanham, MD

J. C. Danko, U. Tennessee, Knoxville, TN

R. Duncan, Combustion Engineering, Inc., Windsor, CT

M. Fox, APTECH, Sunnyvale, CA

Y. S. Garud, S. Levy, Inc., Campbell, CA

F. Garzarolli, KWU, Erlangen, West Germany

B. M. Gordon, General Electric Co., San Jose, CA

S. D. Harkness, Bettis Atomic Power Laboratory, West Mifflin, PA

D. Harrison, USDOE, Germantown, MD

M. E. Indig, General Electric Co., Pleasanton, CA

H. S. Isaacs, Brookhaven National Laboratory, Upton, NY

R. H. Jones, Battelle Pacific Northwest Laboratory, Richland, WA

J. N. Kass, Lawrence Livermore National Laboratory, Livermore, CA

L. Ljungberg, ASEA-ATOM, Vasteras, Sweden

C. D. Lundin, U. Tennessee, Knoxville, TN

D. D. Macdonald, SRI International, Menlo Park, CA

H. Metha, General Electric Co., San Jose, CA

R. A. Oriani, U. Minnesota, Minneapolis, MN

S. Ranganath, General Electric Co., San Jose, CA

E. J. Rowley, Commonwealth Edison Co., Chicago, IL

P. M. Scott, Framatom, Paris, France.

S. Smialowska, Ohio State U., Columbus, OH

D. M. Stevens, Lynchburg Research Center, Babcock & Wilcox Co., Lynchburg, VA

W. A. Van Der Sluys, Research & Development Division, Babcock & Wilcox Co., Alliance, OH

E. Venerus, Knolls Atomic Power Laboratory, Schenectady, NY

J. R. Weeks, Brookhaven National Laboratory, Upton, NY

D. Winkel,Teleco Oil Field Services, Meriden, CN

A. W. Zeuthen, Long Island Lighting Co., Wading River, NY